The cosmic microwave background bispectrum from the non-linear evolution of the cosmological perturbations

Cyril Pitrou

E-mail: `cyril.pitrou@port.ac.uk`
Institute of Cosmology and Gravitation, Dennis Sciama Building, Burnaby
Road, Portsmouth, PO1 3FX, United Kingdom,

Jean-Philippe Uzan

E-mail: `uzan@iap.fr`
Institut d'Astrophysique de Paris, UMR7095 CNRS, Université Pierre & Marie
Curie - Paris, 98 bis bd Arago, 75014 Paris, France,

Francis Bernardeau

E-mail: `francis.bernardeau@cea.fr`
CEA, IPhT, 91191 Gif-sur-Yvette cédex, France,
CNRS, URA-2306, 91191 Gif-sur-Yvette cédex, France.

Abstract. This article presents the first computation of the complete
bispectrum of the cosmic microwave background temperature anisotropies arising
from the evolution of all cosmic fluids up to second order, including neutrinos.
Gravitational couplings, electron density fluctuations and the second order
Boltzmann equation are fully taken into account. Comparison to limiting cases
that appeared previously in the literature are provided. These are regimes for
which analytical insights can be given. The final results are expressed in terms
of equivalent f_{NL} for different configurations. It is found that for moments up to
$\ell_{\max} = 2000$, the signal generated by non-linear effects is equivalent to $f_{\mathrm{NL}} \simeq 5$
for both local-type and equilateral-type primordial non-Gaussianity.

1. Introduction

The Cosmic Microwave Background (CMB) anisotropies are now observed with a
high precision and have become a key observation of modern cosmology. They are in
particular very precious to constrain the theories of the primordial Universe [1]. So
far the temperature anisotropies have been found to have statistical properties that
are compatible with Gaussian statistics [1]. The CMB data can therefore entirely be
captured in its power spectrum and the latter has been used to set constraints on
the cosmological parameters and on the shape of the inflationary potential. There is
hope however that future observations such as Planck [2], that will provide better data

on the statistical properties of the temperature and polarization fields, open a new window on the physics of the early Universe with the use of higher-order statistical properties of the CMB sky such as its bispectrum.

In the analysis of those data, one should keep in mind though that the properties of the CMB temperature and polarization anisotropies depend both on the properties of the initial conditions and on their evolution. As long as measurements are restricted to second-order statistics such as the angular correlation function or the power spectra, a linear perturbation theory suffices, for the required precision, to relate the (2-dimensional) angular power spectrum to the (3-dimensional) initial power spectrum of the metric perturbations at the end of inflation. It has thus been understood that the characteristic features observed in the CMB temperature spectrum originate from the developments of acoustic oscillations encoded in the linear transfer [3, 4] function while its overall amplitude and its scale dependence are fixed by the initial power spectrum, the shape of which agrees with the predictions from an inflationary era [5, 6]. At this level of description, all aspects are now fully understood and is part of textbooks [7, 8, 9, 10, 11, 12] and since the metric and matter perturbations are linearized, any model that predicts Gaussian initial conditions, as standard single field inflation, is expected to produce Gaussian statistical properties for the CMB temperature field.

In general bispectra arise whenever non-linear mode couplings are at play during the cosmological evolution and general relativity being in essence a non-linear field theory, deviations from Gaussianity are expected to be ubiquitous, arising either from the inflationary era (and thus called primordial non-Gaussianity) or from the post-inflationary evolution. Gravity mediated couplings are however generally small and in full agreement with the current data that clearly favors only mild non-Gaussianities if any [1]. In particular, it is now widely accepted that standard single field inflation cannot produce significant non-Gaussianities since its amplitude is mostly dictated by gravity induced couplings [13]. On the other hand, significant deviations from Gaussianity can arise from non-standard kinetic terms, for which models based on the Dirac-Born-Infeld action are typical models [14] or in the context of of multiple-field inflation specially when non-gravity type couplings are at play [15, 16, 17, 18, 19, 20, 21, 22]. It is therefore generally admitted that non-Gaussianity searches can open a window on the details of the inflationary mechanism at work in the early Universe (see Refs. [23, 24, 25] for general reviews).

The level with which primordial non-Gaussianity could actually be detected is however still largely debated, mainly because this source of non-Gaussianity is in "competition" with the couplings induced by non-linear effects throughout the whole recombination and photon propagation processes. This has motivated a series of general studies aiming at characterizing the bispectrum [26, 27, 28, 29, 30, 31, 32, 33, 34, 35, 36, 37, 38, 39, 40, 41, 42] and even the trispectrum [16, 43, 44] to be expected from the observation made by CMB experiments. While the identification of the mode couplings (at the quantum level) during the inflationary phase has been set on secure grounds [13, 45, 46, 47, 48], the evolution of the cosmological perturbations during the post-inflationary era is still largely unexplored, the primordial statistical properties being often related to the observed statistical properties only through a linear transfer function. However, in order to relate the angular bispectrum of the observed CMB to the spatial bispectrum of the metric perturbations at the end of inflation, one needs to derive transfer functions up to second order that incorporate all type of couplings.

Effect	**Linear evolution**	**Non-linear evolution**
Primordial	Primordial power spectrum $P(k)$	Primordial f_{NL}
Primary (early)	Sachs-Wolfe and Doppler effects	This article
Secondary (late)	Integrated Sachs-Wolfe effect, reionization	Lensing-ISW correlation

Table 1. Classification of the linear and non-linear effects.

The work we present in this article is the end result of a task which was initiated in Ref. [49], that was followed by some partial reanalysis [35, 50, 51], In this article we described what we thought is the main mechanism at play for the generation of the bispectra at small angular scales and for which we could give some physical insights. The present article extends this analysis using the theoretical developments of the non-linear perturbation theory described in Refs. [52, 53, 54], and in particular concerning the second order Boltzmann equation that we need in order to describe the evolution of radiation and neutrinos. Its goal is three-fold: (i) to support the predictions and analytic understanding obtained on small scales in Ref. [49] by a full numerical integration of the second order Boltzmann equation, *without neglecting any term*, (ii) to compute the expected bispectrum on intermediate scales, and (iii) to revisit the large-scale behaviour of the bispectrum which has been presented in the previous literature [32, 40, 55]. We emphasize that the amplitude of this non-Gaussianity is completely fixed once the amplitude and power spectrum of the first order scalar perturbations are constrained so that this offers a definite prediction of the minimal amount of non-Gaussianity expected in any CMB observation, that is provided Einstein theory remains a good description of gravity.

Let us mention that our present analysis refines our previous descriptions by classifying the evolution effects, linear or not, in two categories. First, the *primary* or *early* effects arise from the evolution of the perturbations in the radiation dominated era after horizon crossing, during recombination between protons and electrons and until the potentials are constant in their linear evolution. Then *secondary* or *late* effects arise at late time when the potential starts to evolve due the late time acceleration of the Universe or due to reionisation effects (see Ref. [56] and references therein). This separation is unambiguous for the linear evolution and is therefore pertaining to the power spectrum computation but also to the calculation of the bispectrum that mix linear and second order source terms. This is actually clear from Fig. 1 below, and it is summarized in table 1. This present work focuses on the non-linear evolution of the field during the early period and the resulting bispectra it induces. In particular we compute the shape, amplitude and bispectrum of the temperature anisotropies‡ due to these effects and eventually compare them to secondary sources, and specifically the ISW-lensing effects, and to primordial coupling effects (through standard parameterizations). In this work the non-linear evolution of the fluids, including neutrinos, is therefore treated exactly up to second-order in the linear perturbations until reionization is complete. That includes of course the use of the second order Boltzmann equation. Adiabatic initial conditions are also assumed. All the results described here can actually be reproduced from a *Mathematica* code

‡ Note that these results actually depend on the actual definition of the temperature one uses (see the discussion of § 4.1). This is due to the spectral distortion that second order effects necessarily induce as described in Ref. [57].

which is freely available – with its documentation – on the webpage [58].

The article is organized as follows. Section 2 describes the main concepts of the non-linear cosmological perturbation theory while all equations are gathered in Appendix A. Then, in Section 3 we determine the initial conditions for both the metric variables and cosmic fluids (baryon, cold dark matter, photons, neutrinos). In Section 4 we describe, after a careful definition of the temperature in § 4.1, the numerical integration based on the flat sky approximation presented in Section 3. The numerical results concerning the bispectrum are discussed in Section 5 while in Section 6 we provide an analytical understanding of these results in various limiting cases.

2. Non-linear Perturbation Theory

We follow Ref. [53] for the notation. This section summarizes our main choices and conventions and we refer the reader to the latter reference for any further details. We first detail the description of the metric in § 2.1, of the matter fields in § 2.2 and then describe the structure of the perturbation equations in § 2.3.

2.1. Metric perturbations

At lowest order, we assume that the Universe is well described by a Friedmann-Lemaître (FL) space-time with Euclidean spatial sections and with scale factor a. The Universe is then described by a perturbed space-time around this FL background. In the Newtonian gauge (often also named Poisson gauge), the form of the perturbed metric is then given by

$$\mathrm{d}s^2 = g_{\mu\nu}\mathrm{d}x^\mu\mathrm{d}x^\nu \tag{2.1}$$
$$= a(\eta)^2\big\{-(1+2\Phi)\mathrm{d}\eta^2 + 2B_I\mathrm{d}x^I\mathrm{d}\eta + [(1-2\Psi)\delta_{IJ} + 2H_{IJ}]\mathrm{d}x^I\mathrm{d}x^J\big\},$$

with $\partial^I B_I = \partial^I H_{IJ} = H^I_{\ I} = 0$. Here, indices of the type $I, J, K \ldots$ are spatial coordinates indices running from 1 to 3, and η is the conformal time. We also define the comoving Hubble factor $\mathcal{H} = a'/a$ where a prime denotes a derivative with respect to η. Each of the perturbation variables has an order by order expansion of the type [59]

$$X = \bar{X} + X^{(1)} + \frac{1}{2}X^{(2)}. \tag{2.2}$$

In the case of metric perturbations, the definition is made such that their background value vanishes. Additionally, since vector modes fail to be generated at first order in the standard models of inflation [5, 9, 10], we only consider the second order vector modes $B_I^{(2)}$. Similarly, the amplitude of first order tensor modes (i.e. gravitational waves) is expected to be sufficiently low [60] so that we can safely neglect $H_{IJ}^{(1)}$, and we will consider only $H_{IJ}^{(2)}$.

2.2. Describing the matter content

In the concordance model of cosmology, the matter content of the Universe includes relativistic particles (radiation (photons), neutrinos) and non relativistic particules, which fall either in the category of baryons or cold dark matter. Once the equation of state for each species is specified, the background energy density is sufficient to characterize its state. They are denoted $\bar{\rho}_\nu$, $\bar{\rho}_\mathrm{r}$, $\bar{\rho}_\mathrm{c}$ and $\bar{\rho}_\mathrm{b}$ for neutrinos, radiation,

cold dark matter and baryons, respectively. Usually the (perfect) fluids contained in the Universe are characterized in the perturbed Universe by their energy density but also by their velocity. However this is not possible for relativistic particles and, in order to describe photons and neutrinos, we need to rely on a kinetic description based on the moments of their *distribution function*. We will thus describe the fluids as a special case of this statistical description when only the two first moments, which are related to the energy density and the velocity [53], are needed.

2.2.1. The moments of species In general the moments of the distribution function are defined according to the spatial part of a local Minkowski space-time which itself is defined at any point of the space-time manifold by the value of a tetrad field. They are also taken with respect to an azimuthal direction that we arbitrarily align with a given Fourier mode when working out their spatial dependence in Fourier space. We thus describe the radiation with the brightness moments $\mathcal{I}_\ell^{m(1)}(\mathbf{k}, \eta)$ and $\mathcal{I}_\ell^{m(2)}(\mathbf{k}, \eta)$, but also with the moments describing its polarization which are separated into the electric-type moments $\mathcal{E}_\ell^{m(1)}(\mathbf{k}, \eta)$ and $\mathcal{E}_\ell^{m(2)}(\mathbf{k}, \eta)$, and the magnetic type moments $\mathcal{B}_\ell^{m(2)}(\mathbf{k}, \eta)$ (which appear only at second order since we have assumed that the first order vector and tensor modes can be neglected). The polarization of radiation is generated through the interactions with baryons while the neutrinos, being collisionless, develop no polarization. As a consequence, we only need the brightness moments $\mathcal{N}_\ell^{m(1)}(\mathbf{k}, \eta)$ and $\mathcal{N}_\ell^{m(2)}(\mathbf{k}, \eta)$ to describe them (we also assume that the three species of neutrinos are massless and we describe them altogether though their mass splitting can have some interesting cosmological implications [61, 62]).

The matter species, i.e. baryons and cold dark matter, are described by perfect fluids. The perturbation of their energy densities is defined according to the decomposition (2.2). The spatial moments of the velocities of these fluids are noted v_m with $m = -1, 0, 1$ and their perturbation is also defined according to Eq. (2.2) with no background value thanks to the symmetries of the background space-time, which imply that all fluids have the four-velocity $\bar{u}^\mu = \frac{1}{a}\delta_0^\mu$ since no preferred direction exists. Furthermore, since the first order vector modes are not generated at first order, we have $v_{\pm 1}^{(1)} = 0$.

Additionally, it will prove more convenient to work also with the moments of the vector and tensor perturbations, that is with $\Phi_{\pm 1}^{(2)}$ and $H_{\pm 1}^{(2)}$ instead of B_I and H_{IJ}. Again, we refer to Ref. [53] for the exact definitions which are inspired from Ref. [63].

2.2.2. Stress-energy tensor For a perfect fluid, the stress-energy tensor is given by

$$T_{\mu\nu} = \rho u_\mu u_\nu + P\left(g_{\mu\nu} + u_\mu u_\nu\right), \tag{2.3}$$

where the pressure is related to the energy density by an equation of state $P = w\rho$. We can see on this expression of the stress-energy tensor that we neglect the anisotropic stress and it thus applies for baryons and cold dark matter only. For radiation and neutrinos, the stress-energy tensor can be constructed from the distribution function and it is thus possible to relate its expression to the moments of the brightness (see Ref. [53] for instance).

2.3. Field equations

2.3.1. Structure of the equations Three equations are essential to understand the evolution of perturbations of the radiation. First, we need the Einstein equation

$G_{\mu\nu} = \kappa T_{\mu\nu}$ with $\kappa = 8\pi G$, in order to relate the perturbations of the metric to the ones of the different matter species. Then, the evolution of the distribution functions is dictated by the Boltzmann equation from which one can extract the evolution hierarchy of its moments. Finally, since the collision rate between photons and baryons is proportional to the fraction of free electrons, x_e, which is governing the recombination process, we need to derive the evolution equation of x_e up to the first order in the perturbations. These three sets of equations are detailed in Appendix A.

At linear order, the evolution equations are partial differential equations which are by construction linear in the perturbation variables. They formally take the form

$$\mathcal{D}_i[X_j^{(1)}] = 0\,, \tag{2.4}$$

where the $X_j^{(1)}$ is the set of first order perturbation variables and $\mathcal{D}_i$ the set of differential operators acting on them. At second order the purely second order perturbation variables satisfy the same differential equations, but supplemented with source terms which are quadratic in the first order variables, i.e. they are of the form

$$\mathcal{D}_i[X_j^{(2)}] = \mathcal{S}_i[X_j^{(1)}], \tag{2.5}$$

where the terms $\mathcal{S}_i$ are operators (possibly differential) quadratic in their arguments. It is thus sufficient to write down the second order equations, that is the linear operators $\mathcal{D}_j$ and the source terms $\mathcal{S}_i$, in order to fully specify both the first and the second order equations.

2.3.2. Structure of the solutions At first order, the space of solutions is spanned by the linear combinations of independent solutions since the operators $\mathcal{D}_i$ are linear. Then, the choice of the initial conditions selects a particular solution in this vector space of solutions. However, at second order, the space of solutions is spanned by the linear combinations of the same independent solutions to which a particular solution has to be added, thanks to the non vanishing source terms $\mathcal{S}_i$ which break the linearity, so that it belongs to an affine space instead of a vector space. The choice of this particular solution is arbitrary so that we can decide to take the one which vanishes deep in the radiation dominated era. This particular solution will then be physically interpreted as the cumulative effect of the sources and this is actually what we mean when we compare the effects of non-linear evolution to those of the linear evolution, the latter being the solutions of the homogeneous equation. As explained in the introduction, the goal of this article is to assess the importance of the non-linear evolution effects on the temperature bispectrum with respect to the linear evolution effects which are now well under control from a theoretical and numerical point of view.

2.3.3. Fourier space and convention From a technical point of view, we will solve numerically the evolution equations in Fourier space. We define the Fourier transform of any function $X(\mathbf{x}, \eta)$ as

$$X(\mathbf{k}, \eta) = \int \frac{\mathrm{d}^3\mathbf{x}}{(2\pi)^{3/2}} X(\mathbf{x}, \eta)\mathrm{e}^{-\mathrm{i}\mathbf{k}\cdot\mathbf{x}} \tag{2.6}$$

and we will use the expression of the Fourier transform of a product as the convolution

$$[XY](\mathbf{k}) = \mathcal{K}\{X(\mathbf{k}_1)Y(\mathbf{k}_2)\}\,, \tag{2.7}$$

hence introducing the short hand notation

$$\mathcal{K}\{\dots\} \equiv \int \frac{\mathrm{d}^3\mathbf{k}_1 \mathrm{d}^3\mathbf{k}_2}{(2\pi)^{3/2}} \delta_D^3(\mathbf{k}_1 + \mathbf{k}_2 - \mathbf{k}) \dots,$$

where δ_D^3 is the 3-dimensional Dirac distribution.

3. Initial conditions

Since both radiation and neutrinos are relativistic, the ratio of their energy densities is conserved during the cosmological evolution, and we define the fraction of radiation among the relativistic species by $f_{\mathrm{r}} \equiv \bar{\rho}_{\mathrm{r}}/(\bar{\rho}_{\mathrm{r}} + \bar{\rho}_\nu)$. Similarly, cold dark matter and baryons being pressureless and coupled to gravity universally [64], the ratio of their energy densities is also conserved. We also define

$$R = \frac{3}{4} \frac{\bar{\rho}_{\mathrm{b}}}{\bar{\rho}_{\mathrm{r}}}. \tag{3.1}$$

In this section focusing on the initial conditions, all expressions are meant to hold only at an initial time η_{init}. We thus omit to specify it in order to simplify the notation. We now give the initial conditions for the matter perturbation variable in § 3.1 and the geometry perturbation variables in § 3.2, both at first and second orders.

3.1. Initial conditions for the matter variables

We only consider in this article adiabatic initial conditions since isocurvature modes are highly constrained observationnally [65] but also because the single field models of inflation [9, 10] predict adiabatic initial conditions. The link between isocurvature modes and multiple-field models remains to be investigated in depth [18, 66].

For adiabatic initial conditions, the velocity of all matter species is negligible both at the first and at second orders. It is indeed suppressed by a factor $k\eta_{\mathrm{init}}$ compared to Φ_{init}. We thus take the initial condition

$$v_m^{(1)} = v_m^{(2)} = 0, \quad \text{with} \quad m = -1, 0, 1 \tag{3.2}$$

for baryons and cold dark matter and we take

$$\mathcal{I}_1^{m(1)} = \mathcal{N}_1^{m(1)} = \mathcal{I}_1^{m(2)} = \mathcal{N}_1^{m(2)} = 0, \tag{3.3}$$

for radiation and neutrinos. Adiabaticity also implies that the ratios between $\rho_{\mathrm{b}}^{1/3}$, $\rho_{\mathrm{c}}^{1/3}$, $\rho_{\mathrm{r}}^{1/4}$ and $\rho_\nu^{1/4}$ remain constant. We deduce the following initial conditions§

$$\frac{1}{3}\frac{\rho_{\mathrm{c}}^{(1)}}{\bar{\rho}_{\mathrm{c}}} = \frac{1}{3}\frac{\rho_{\mathrm{b}}^{(1)}}{\bar{\rho}_{\mathrm{b}}} = \frac{1}{4}\mathcal{I}_0^{0(1)}, \tag{3.4a}$$

$$\frac{1}{3}\frac{\rho_{\mathrm{c}}^{(2)}}{\bar{\rho}_{\mathrm{c}}} = \frac{1}{3}\frac{\rho_{\mathrm{b}}^{(2)}}{\bar{\rho}_{\mathrm{b}}} = \frac{1}{4}\mathcal{I}_0^{0(2)} - \left[\frac{1}{4}\mathcal{I}_0^{0(1)}\right]^2, \tag{3.4b}$$

$$\mathcal{I}_0^{0(1)}(k) = \mathcal{N}_0^{0(1)}(k), \tag{3.4c}$$

$$\mathcal{I}_0^{0(2)}(k) = \mathcal{N}_0^{0(2)}(k). \tag{3.4d}$$

§ $\mathcal{I}_0^0$ is not exactly the energy density since the frame used to define the multipoles is not necessarily comoving with the species. However the difference are quadratic in the velocity field, mainly because it arises from boost factors, and it is thus not important for the initial conditions. See Refs. [53, 67] for the link between these two quantities.

Now, using the Poisson equation (A.1) deep in the radiation era, we can relate these initial conditions to those of the metric perturbations as

$$\mathcal{I}_0^{0(1)} = -2\Phi^{(1)}, \tag{3.5a}$$

$$\mathcal{I}_0^{0(2)} = -2\Phi^{(2)} + 8\Phi^{(1)2}. \tag{3.5b}$$

Additionally, the presence of neutrinos implies that $\frac{\mathcal{H}^2}{k^2}\mathcal{N}_2^0\|$ does not vanish and this term is required in order to determine the initial conditions for the perturbations of the two gravitational potentials since $\Phi - \Psi$ is proportional to $\mathcal{N}_2^0 + \mathcal{I}_2^0$; see Eq. (A.3). Appendix C details the initial conditions satisfied by the quadrupoles $\mathcal{I}_2^{0(2)}$, $\mathcal{N}_2^{0(1)}$ and $\mathcal{N}_2^{0(2)}$ while we always have $\mathcal{I}_2^{0(1)} = 0$.

3.2. Initial conditions for the metric variables

As previously, we fix the initial conditions deep in the radiation dominated era for super-Hubble modes, so that we can expand all our equations in terms of $k\eta_{\text{init}} \ll 1$. For adiabatic perturbations, we recall that on super-Hubble scales the comoving curvature perturbation is conserved. Its expressions at first and second orders are [68, 69]

$$\mathcal{R}^{(1)} = \Psi^{(1)} + \frac{2}{3(1+w)\mathcal{H}}\left[\Psi'^{(1)} + \mathcal{H}\Phi^{(1)}\right], \tag{3.6a}$$

$$\mathcal{R}^{(2)} = \Psi^{(2)} + \frac{2}{3(1+w)\mathcal{H}}\left[\Psi'^{(2)} + \mathcal{H}\Phi^{(2)} - 4\mathcal{H}\Phi^{(1)2} - \frac{\Psi^{(1)'2}}{\mathcal{H}} - 4(\Phi^{(1)} - \Psi^{(1)})\Psi^{(1)'}\right]$$
$$+ \left(1 + 3c_s^2\right)\left[\frac{\rho^{(1)}}{3(1+w)\bar{\rho}}\right]^2 + \frac{4}{3(1+w)}\frac{\rho^{(1)}}{\bar{\rho}}\Psi^{(1)}, \tag{3.6b}$$

where w and c_s^2 are the equation of state and the adiabatic speed of sound of the total fluid. Deep in the radiation era the properties of the total fluid are close to the radiation+neutrinos fluid since $\bar{\rho}_{\text{m}} \ll \bar{\rho}_{\text{r}}$ and $w = c_s^2 = 1/3$. At first order, we obtain the initial conditions [70]

$$\left[1 + \frac{4}{15}(1 - f_{\text{r}})\right]\Phi^{(1)} = \frac{2}{3}\mathcal{R}^{(1)}, \tag{3.7a}$$

$$\Psi^{(1)} - \Phi^{(1)} = \frac{2}{5}(1 - f_{\text{r}})\Phi^{(1)}, \tag{3.7b}$$

which in particular implies $\mathcal{R}^{(1)} = \Psi^{(1)} + \Phi^{(1)}/2$. At second order, we obtain

$$\Psi^{(2)} = \frac{2}{3}\left(\frac{3}{2}\Phi^{(1)2} + 2\Phi^{(1)}\Psi^{(1)}\right) + \frac{1}{3}S_3 + \frac{2}{3}\mathcal{R}^{(2)}, \tag{3.8a}$$

$$\Phi^{(2)} = \frac{2}{3}\left(\frac{3}{2}\Phi^{(1)2} + 2\Phi^{(1)}\Psi^{(1)}\right) - \frac{2}{3}S_3 + \frac{2}{3}\mathcal{R}^{(2)} \tag{3.8b}$$

where

$$S_3 = \tilde{S}_3 - \frac{3}{5}\mathcal{H}^2\Delta^{-1}\left[f_{\text{r}}\mathcal{I}_2^{0(2)} + (1 - f_{\text{r}})\mathcal{N}_2^{0(2)}\right], \tag{3.9}$$

‖ Note that the quadrupole moments, that is the moments with $\ell = 2$ ($\mathcal{N}_2^m$ and $\mathcal{I}_2^m$) are different from the anisotropic stress of neutrinos and photons [67]. In fact they match only if the frame in which the moments are taken is aligned with the velocity of the species considered.

$$\tilde{S}_3 = -4\Psi^{(1)2} - 2\Phi^{(1)2}$$
$$- \Delta^{-1} \left[\partial_I(\Psi^{(1)} + \Psi^{(1)})\partial^I(\Psi^{(1)} + \Phi^{(1)}) + 2\Psi^{(1)}\Delta\Phi^{(1)} \right]$$
$$+ 3(\Delta\Delta)^{-1}\partial_I\partial_J \left[\partial^I(\Psi^{(1)} + \Phi^{(1)})\partial^J(\Psi^{(1)} + \Phi^{(1)}) + 2\Psi^{(1)}\partial_I\partial_J\Phi^{(1)} \right]. \quad (3.10)$$

It can also be recast in the following set of two initial conditions

$$\left[1 + (1 - f_r)\frac{4}{15} \right] \Phi^{(2)} = \frac{2}{3} \left\{ \frac{3}{2}\Phi^2 + 2\Phi\Psi + \mathcal{R}^{(2)} - S_3 \right\}, \quad (3.11a)$$

$$\Psi^{(2)} - \Phi^{(2)} = S_3. \quad (3.11b)$$

In order to make link with previous works [26], note that in the case where there are no neutrinos ($f_r = 1$) we obtain

$$\Phi^{(1)} = \Psi^{(1)} = \frac{2}{3}\mathcal{R}^{(1)}, \quad (3.12a)$$

$$\Psi^{(2)} = \frac{2}{3}\mathcal{R}^{(2)} + \Psi^{(1)2} - \Delta^{-1}\left[\partial_I\Psi^{(1)}\partial^I\Psi^{(1)} \right] + 3\Delta^{-2}\partial^J\partial_I\left[\partial_J\Psi^{(1)}\partial^I\Psi^{(1)} \right], \quad (3.12b)$$

$$\Phi^{(2)} = \Psi^{(2)} + 4\Psi^{(1)2} + 3\Delta^{-1}\left[\partial_I\Psi^{(1)}\partial^I\Psi^{(1)} \right] - 9\Delta^{-2}\partial^J\partial_I\left[\partial_J\Psi^{(1)}\partial^I\Psi^{(1)} \right]. \quad (3.12c)$$

For the vector and tensor modes, we have argued that they are respectively purely decaying modes or of negligible amplitude at first order, so that

$$\Phi^{(1)}_{\pm 1} = H^{(1)}_{\pm 1} = 0. \quad (3.13)$$

At second order, vector and tensor type perturbations exclusively arise from the integrated contribution of the quadratic sources so that they also vanish at sufficiently early times. We thus have

$$\Phi^{(2)}_{\pm 1} = H^{(2)}_{\pm 1} = 0. \quad (3.14)$$

3.3. Primordial non-Gaussianity and $f_{\rm NL}$

In the previous section, we have not specified the value of $\mathcal{R}^{(2)}$. Indeed this is what we would like to constrain by measuring the level of non-Gaussianity since different models of inflation have different predictions. In general, theoretical predictions are given in terms of the spectrum and of the bispectrum of $\mathcal{R}$ related to the 2- and 3-point functions by

$$\langle \mathcal{R}(\mathbf{k}_1)\mathcal{R}(\mathbf{k}_2) \rangle = \langle \mathcal{R}^{(1)}(\mathbf{k}_1)\mathcal{R}^{(1)}(\mathbf{k}_2) \rangle = \delta^3_D(\mathbf{k}_1 + \mathbf{k}_2) P_{\mathcal{R}}(k_1), \quad (3.15)$$

and

$$\langle \mathcal{R}(\mathbf{k}_1)\mathcal{R}(\mathbf{k}_2)\mathcal{R}(\mathbf{k}_3) \rangle = \frac{1}{2}\langle \mathcal{R}^{(1)}(\mathbf{k}_1)\mathcal{R}^{(1)}(\mathbf{k}_2)\mathcal{R}^{(2)}(\mathbf{k}_3) \rangle + \text{sym.}$$
$$= \delta^3_D(\mathbf{k}_1 + \mathbf{k}_2 + \mathbf{k}_3) \ f^{\mathcal{R}}_{\rm NL} \ F(\mathbf{k}_1, \mathbf{k}_2, \mathbf{k}_3), \quad (3.16)$$

where $P_{\mathcal{R}}(k)$ is the primordial power spectrum and $F(\mathbf{k}_1, \mathbf{k}_2, \mathbf{k}_3)$ is a function which specifies the shape of the primordial non-Gaussianity and $f^{\mathcal{R}}_{\rm NL}$ is its amplitude. Each possible type of primordial non-Gaussianity is characterized by a function $F(\mathbf{k}_1, \mathbf{k}_2, \mathbf{k}_3)$, and these functions are normalized such that they all have the same value in the Fourier configuration $k_1 = k_2 = k_3$.

Different limiting cases can be found in the literature [71], the main one being the non-Gaussianity of the *local type* for which

$$F_{\text{loc}}(\mathbf{k}_1, \mathbf{k}_2, \mathbf{k}_3) = 2P_{\mathcal{R}}(k_1)P_{\mathcal{R}}(k_2) + 2\,\text{sym.} \tag{3.17}$$

In this case, it is equivalent to specify that

$$\mathcal{R}^{(2)}(\mathbf{k}) = 2\mathcal{K}\left\{f_{\text{NL}}^{\mathcal{R}}\mathcal{R}^{(1)}(\mathbf{k}_1)\mathcal{R}^{(1)}(\mathbf{k}_2)\right\} \tag{3.18}$$

in Fourier space. In particular, it has been shown [13] that for slow-rolling single field inflationary models

$$\mathcal{R}^{(2)} \simeq -2\mathcal{R}^{(1)2}\,, \tag{3.19}$$

that is $f_{\text{NL}}^{\mathcal{R}} \simeq -1$. Note that this is equivalent to impose that $f_{\text{NL}}^{\mathcal{R}_M} \simeq 0$ with $\exp(-2\mathcal{R}_M) \equiv 1 - 2\mathcal{R}$ [13]. This is the initial condition that we shall assume in this work since we want to study the effects of evolution in the pursuit of non-Gaussianity and want to consider the minimum amount of primordial non-Gaussianity (see however the discussion of § 3.4 below).

Note also that most expressions are given in terms of the power-spectrum of the gravitational potential $\Phi^{(1)}$ rather than $\mathcal{R}^{(1)}$. The two power spectra are easily related thanks to

$$P_{\Phi}(k) = \frac{4}{9}\frac{1}{\left[1 + \frac{4}{15}(1 - f_{\text{r}})\right]^2}P_{\mathcal{R}}(k)\,. \tag{3.20}$$

Similarly, the primordial non-Gaussianity is more often expressed in terms of a f_{NL} parameter which is related to Φ rather than $\mathcal{R}$. In order to be consistent with previous literature in which neutrinos were not included at second order, we define f_{NL}^{Φ} through

$$\Phi^{(2)}(\mathbf{k}) = -2\mathcal{K}\left\{f_{\text{NL}}^{\Phi}\frac{3}{5}\left[\frac{3}{2}\left(1 + \frac{4}{15}(1 - f_{\text{r}})\right)\right]\Phi^{(1)}(\mathbf{k}_1)\Phi^{(1)}(\mathbf{k}_2)\right\}\,, \tag{3.21}$$

which is inspired from Eq. (3.11a) when quadratic terms are ignored, that is when the relation between $\Phi^{(2)}$ and $\mathcal{R}^{(2)}$ is approximated to be linear, which is a valid approximation for large primordial non-Gaussinities. This is the non-Gaussianity parameter that we will discuss in the rest of this article. Historically, the definition (3.21) was made for $f_{\text{r}} = 1$, and since the matter dominated era potential is related to the primordial one by $\Phi_{\text{mat}}^{(1)} = \frac{9}{10}\Phi_{\text{init}}^{(1)}$ on large scales, then we would obtain

$$\Phi_{\text{mat}}^{(2)}(\mathbf{k}) = -2\mathcal{K}\left\{f_{\text{NL}}^{\Phi}\Phi_{\text{mat}}^{(1)}(\mathbf{k}_1)\Phi_{\text{mat}}^{(1)}(\mathbf{k}_2)\right\}\,. \tag{3.22}$$

It is useful to notice that when we consider the neutrinos ($f_{\text{r}} \neq 1$) for the concordance model [1]

$$\frac{3}{5}\left[\frac{3}{2}\left(1 + \frac{4}{15}(1 - f_{\text{r}})\right)\right]\left(\Phi^{(1)}\right)^2 \simeq 0.99\left(\Phi^{(1)}\right)^2\,, \tag{3.23}$$

and thus, the same type of relation holds when considering neutrinos, but deep in the radiation dominated era.

Another interesting family of non-Gaussian initial conditions, motivated by models such DBI inflation, is of the *equilateral type* where the function F peaks when $k_1 = k_2 = k_3$. The expression for such type of non-Gaussianity is given in Ref. [72] and reads

$$F_{\text{equi}}(\mathbf{k}_1, \mathbf{k}_2, \mathbf{k}_3) = 6\left\{-P_{\mathcal{R}}(k_1)P_{\mathcal{R}}(k_2) + 2\,\text{sym.} - 2\left[P_{\mathcal{R}}(k_1)P_{\mathcal{R}}(k_2)P_{\mathcal{R}}(k_3)\right]^{2/3}\right.$$
$$\left. + P_{\mathcal{R}}^{1/3}(k_1)P_{\mathcal{R}}^{2/3}(k_2)P_{\mathcal{R}}(k_3) + 5\,\text{sym.}\right\}\,. \tag{3.24}$$

Similarly to what has been done in Eq. (3.21) we can also define a f_{NL}^{Φ} for the equilateral configuration. The local and equilateral type non-Gaussianities are interesting from a technical point a view, since there analytical expression in function of k_1, k_2 and k_3 is factorizable in powers of these quantities. This implies that the optimal estimator, that we need to build to constrain this type of primordial non-Gaussianity, is faster than for a general shape of the primordial non-Gaussianity [31]. Even if the true primordial non-Gaussianity is not strictly of the local or equilateral type, it can be approximated by these ideal cases in order to produce constraints on the primordial non-Gaussianity in a fast and efficient manner [42].

3.4. Why we can concentrate on $f_{\mathrm{NL}}^{\mathcal{R}} = -1$ and still be general

Let us now stress that as long as one considers the bispectrum, the result is linear in the second order solution. This linearity shall not be confused with the non-linearity of the perturbation equations. Indeed, as long as the initial conditions at first order are identical, the second order initial conditions (3.4b, 3.5b, 3.12b, 3.12c) for the matter and metric perturbations are linear in $\mathcal{R}^{(2)}$. Since the solutions of the second order perturbation equation belong to an affine space, we can always write $f_{\mathrm{NL}}^{\mathcal{R}} \equiv f_{\mathrm{NL\,prim}}^{\mathcal{R}} + f_{\mathrm{NL\,1field}}^{\mathcal{R}}$, where the first quantity refers to the extra primordial non-Gaussianity compared to the standard one-field inflation prediction $f_{\mathrm{NL\,1field}}^{\mathcal{R}}$. It follows that the initial condition for $\mathcal{R}^{(2)}$ satisfies

$$\mathcal{R}^{(2)}(\mathbf{k}) = 2\mathcal{K}\left\{f_{\mathrm{NL\,prim}}^{\mathcal{R}}\mathcal{R}^{(1)}(\mathbf{k}_1)\mathcal{R}^{(1)}(\mathbf{k}_2)\right\} + 2\mathcal{K}\left\{f_{\mathrm{NL\,1field}}^{\mathcal{R}}\mathcal{R}^{(1)}(\mathbf{k}_1)\mathcal{R}^{(1)}(\mathbf{k}_2)\right\},$$

that is $\mathcal{R}^{(2)}(\mathbf{k}) = \mathcal{R}_{\mathrm{prim}}^{(2)}(\mathbf{k}) + \mathcal{R}_{\mathrm{NL\ evolution}}^{(2)}(\mathbf{k})$. All the purely second order variables will thus be decomposed as $X^{(2)}(\mathbf{k}) = X_{\mathrm{prim}}^{(2)}(\mathbf{k}) + X_{\mathrm{NL\ evolution}}^{(2)}(\mathbf{k})$ and the final bispectrum will simply be the superposition of a primordial bispectrum and of the bispectrum induced by the non-linear evolution that is computed in this article.

4. Computation of the spectrum and bispectrum

We adopt the line of sight approach [63, 70, 73, 74, 75] in the resolution of the Boltzmann equation. This consists in considering that the observed brightness in a given direction of the CMB is the sum of the brightness of the emitting sources. It simplifies the numerical implementation since, at least at the first order in perturbations, only lower multipoles contribute to the sources.

In this section, we first discuss the definition of the temperaturre in § 4.1 and then describe the expression of the emitting sources in § 4.2 (after having defined our choice of definition for the temperature in § 4.1). Then we use a flat sky approximation (to be distinguished from the Limber approximation which is an extra approximation, which can be made or not) in order to simplify the numerical integration both for the spectrum in § 4.2 and for the bispectrum in § 4.5. We refer to Ref. [76] for the detailed derivation of the expressions summarized below and for a discussion of their accuracy.

4.1. Defining the temperature

The primary physical quantity related to the distribution function is the brightness, and we need to define the CMB temperature from this quantity. First we define the

brightness temperature fractional perturbation by

$$\Theta \equiv \frac{1}{4}\left(\frac{\mathcal{I}}{\bar{\mathcal{I}}} - 1\right),\tag{4.1}$$

where $\bar{\mathcal{I}} = \bar{\rho}_\gamma$ is the background value of the brightness, from which we can define the *brightness temperature* by $T_\mathcal{I} \equiv \bar{T}(1 + \Theta)$. This definition is inspired from the more general *bolometric temperature* T which is defined by

$$\left(\frac{T}{\bar{T}}\right)^4 \equiv \frac{\mathcal{I}}{\bar{\mathcal{I}}}.\tag{4.2}$$

The brightness temperature and the bolometric temperature agree at the background and first order level. Since the Boltzmann equation is derived in function of the brightness, the brightness temperature is the most straightforward quantity to use, but the bolometric temperature carries more meaning since it is the temperature of the black-body distribution which would have the same energy density as the actual distribution. However, it has be shown [57] that the non-linear dynamics sources a y-type spectral distortion and this would affect the brightness and thus both the brightness and the bolometric temperatures. Following our previous analysis [57], it would be more natural to use the *occupation number temperature* defined as the temperature of a black-body which would have the same number density of photons as the observed distribution (to be contrasted with the bolometric temperature which is the temperature of the black body which carries the same energy density as the observed distribution). It is thus defined by

$$T_N \equiv \frac{T}{(1 + 4y)^{\frac{1}{4}}}.\tag{4.3}$$

Defined like this, this temperature is not affected by spectral distortions since Compton scattering conserves the number of photons in collisions, and it has a non-ambiguous signification with the type of distortions induced by the non-linear collision term [57].

These definitions agree at the background level and at first order in the perturbation so that $C_\ell^{T_\mathcal{I} T_\mathcal{I}} = C_\ell^{TT} = C_\ell^{T_N T_N} \equiv \bar{T}^2 C_\ell^{\Theta\Theta}$. Since they differ at second order in perturbations, we can define three different bispectra, depending on the choice of definition for the temperature. As we shall see in § 5.4, since at lowest order in the spectral distortions [57]

$$T = T_N(1 + y),\tag{4.4}$$

the three bispectra are related to one another so that one only needs to compute one of them. In order for our results to be easily compared with the existing literature, we will use the bolometric temperature. although the occupation number temperature is, at least from a theoretical point of view, more natural to use.

4.2. Emitting sources and transfer functions

Given the definition of the multipoles used in Ref. [53], the brightness temperature emitted by a multipole $\mathcal{I}_\ell^m(\mathbf{k}, \eta)$ is given by

$$\frac{1}{4}Q_\ell^m(\mathbf{k})\mathcal{I}_\ell^m(\mathbf{k}, \eta),\tag{4.5}$$

where we have introduced

$$Q_\ell^m(\mathbf{k}) \equiv N_\ell^{-1} Y_\ell^m(\hat{\mathbf{k}}),\tag{4.6}$$

$\hat{\mathbf{k}}$ being the unit vector in the direction of $\mathbf{k}$ and where

$$N_\ell \equiv i^\ell \sqrt{\frac{2\ell+1}{4\pi}}\,. \tag{4.7}$$

It follows that the total expression of the emitting sources is given by

$$W(\mathbf{k},\eta) \equiv \exp(-\bar{\tau}) \sum_{\ell,m} S_\ell^m(\mathbf{k},\eta) Q_\ell^m(\mathbf{k})\,, \tag{4.8}$$

where $\bar{\tau}$ is the optical thickness which satisfies the integral equation

$$\bar{\tau} = \int_\eta^{\eta_0} d\eta'\, \bar{\tau}'(\eta')\,, \tag{4.9}$$

that is $d\bar{\tau}/d\eta = -\bar{\tau}'$, and where the emitting sources multipoles S_ℓ^m are defined in Appendix B. This expression is valid both at first and at second order, depending on whether we consider the first order or the second order sources. Since we want to determine how the primordial perturbations of the gravitational potential Φ translate into the observed temperature, we are rather interested in the transfer functions defined by

$$w^{(1)}(\mathbf{k},\eta)\Phi(\mathbf{k},\eta_{\mathrm{init}}) \equiv W^{(1)}(\mathbf{k},\eta)\,, \tag{4.10a}$$

$$\mathcal{K}\left\{w^{(2)}(\mathbf{k}_1,\mathbf{k}_2,\eta)\Phi^{(1)}(\mathbf{k}_1,\eta_{\mathrm{init}})\Phi^{(1)}(\mathbf{k}_2,\eta_{\mathrm{init}})\right\} \equiv W^{(2)}(\mathbf{k},\eta)\,. \tag{4.10b}$$

As we shall see, $w^{(1)}(\mathbf{k},\eta)$ and $w^{(2)}(\mathbf{k}_1,\mathbf{k}_2,\eta)$ will be computed numerically. In principle the $\mathcal{I}_\ell^m(\mathbf{k})$ are complex functions, but numerically we prefer to manipulate real numbers and real differential equations. At first order this is not an issue since only the scalar perturbations are non vanishing and $\mathcal{I}_\ell^{0(1)}(\mathbf{k})$ remains unchanged under a rotation of the coordinates system around $\mathbf{k}$, that is about the azimuthal direction used for the spherical harmonics. However, at second order, this is no more the case since for a given ℓ all the allowed m are to be taken into account. In order to perform the integration with real numbers, we thus choose the orientations of $\mathbf{k}_1$ and $\mathbf{k}_2$ such that $\varphi_{\mathbf{k}_1} = \varphi_{\mathbf{k}_2} = 0$, that is $k_{1y} = k_{2y} = 0$. When the azimuthal direction of the spherical harmonics is $\mathbf{k}$, $\mathcal{I}_\ell^{m(1)}(\mathbf{k}_1)$ and $\mathcal{I}_\ell^{m(1)}(\mathbf{k}_2)$ are then computed according to Eq. (A.37), which ensures that they remain real. In the computation of the bispectrum, we will then need a general orientation of $\mathbf{k}_1$ and $\mathbf{k}_2$. It can be obtained by rotating this configuration around the azimuthal direction $\mathbf{k}$ by an angle $\alpha(\mathbf{k}_1,\mathbf{k}_2)$. Defining $\mathcal{I}_\ell^{m(2)}$ in a similar way as Eq. (4.10b),

$$\mathcal{K}\left\{\mathcal{I}_\ell^{m(2)}(\mathbf{k}_1,\mathbf{k}_2,\eta)\Phi^{(1)}(\mathbf{k}_1,\eta_{\mathrm{init}})\Phi^{(1)}(\mathbf{k}_2,\eta_{\mathrm{init}})\right\} \equiv \mathcal{I}_\ell^{m(2)}(\mathbf{k},\eta)\,, \tag{4.11}$$

it can be related to the result of the (real) numerical integration $\mathcal{I}_{\ell\,\mathrm{real}}^m(\mathbf{k}_1,\mathbf{k}_2)$ by

$$\mathcal{I}_\ell^m(\mathbf{k}_1,\mathbf{k}_2) = e^{im\alpha(\mathbf{k}_1,\mathbf{k}_2)}\mathcal{I}_{\ell\,\mathrm{real}}^m(\mathbf{k}_1,\mathbf{k}_2)\,. \tag{4.12}$$

Our notation α refers to the Euler angles.

4.3. Flat sky approximation

In the flat sky approximation, the sky is expanded around a reference line of sight with direction $\hat{\mathbf{r}}$. Any Fourier mode $\mathbf{k}$ can then be split into a component $k_\parallel = k \cdot \hat{\mathbf{r}}$ parallel to the line of sight and a 2-dimensional projection, $\mathbf{k}_\perp = \mathbf{k} - k_\parallel \hat{\mathbf{r}}$, in the plane orthogonal to this line of sight.

While the orientation of the Fourier mode with respect to the line of sight does not matter for the monopole of the brightness ($\ell = 0$), it plays an important role for higher order multipoles ($\ell \geq 1$). Indeed their contribution to the radiation that we receive depends on the orientation of $\mathbf{k}$ with respect to the direction of the flat sky.

The flat sky approximation is independent from the resolution of the Boltzmann equation. We start by solving the first few moments of the emitting sources by integrating a truncated Boltzmann hierarchy, and only after this we use the line of sight method to obtain all the multipoles of the CMB. The flat sky approximation is only used in this final step and proves to be a very good approximation for $\ell > 10$, since the error is much smaller than the cosmic variance, and reaches a percent accuracy beyond $\ell = 100$. Two subcases of the flat sky approximation exist [76]. The Limber approximation corresponds to cases where the sources vary slowly in time and over a wide range of distances along the line of sight. This case is not well suited for CMB except for effects like the late ISW. The second regime corresponds to the thin shell approximation. It relies on the hypothesis that the sources are located in a narrow range of distances. This is the one that we use in this article since it appears to be well suited for primary CMB calculations as illustrated in Fig. 1.

Let us also note that the procedure described in the previous section in order to consider a general orientation of $\mathbf{k}$, $\mathbf{k}_1$ and $\mathbf{k}_2$ with respect to the flat sky can be obtained as follows. First, we align the azimuthal direction $\mathbf{k}$ with the direction $\hat{\mathbf{r}}$ of the flat sky which is chosen as the $\mathbf{z}$ direction of a Cartesian coordinate system. Two other axes $\mathbf{x}$ and $\mathbf{y}$ perpendicular $\mathbf{z}$ can then be defined. We choose $\mathbf{k}_1$ and $\mathbf{k}_2$ to lie in the plane spanned by $\mathbf{z}$ and $\mathbf{x}$. From this particular configuration, we can reach a general configuration by first rotating around $\mathbf{z}$ by an angle α, then by rotating around $\mathbf{y}$ by an angle β, and finally by rotating around $\mathbf{z}$ by an angle γ. These last two rotations enable to reach $\mathbf{k}$ from the direction $\mathbf{z}$. In the notation $Y_\ell^m(\hat{\mathbf{k}})$ of Eq. (4.6), we thus meant $Y_\ell^m(\alpha, \beta)$.

4.4. Spectrum

As usual, the temperature anisotropies can be decomposed in spherical harmonics as

$$\Theta(n^i) = \sum_{\ell m} a_{\ell m} Y_m^\ell(n^i), \tag{4.13}$$

hence defining the coefficients $a_{\ell m}$. The global isotropy of the Universe implies [77, 78] that the 2-point correlation function of Θ can be decomposed as

$$\langle \Theta(n_1^i) \Theta(n_2^i) \rangle = \sum_\ell \frac{2\ell + 1}{4\pi} C_\ell^{\Theta\Theta} P_\ell(\cos\theta) \tag{4.14}$$

where $n_1^i n_{2i} = \cos\theta$ and the brackets refer to an ensemble average or to an average on the sky if Θ is the observed temperature. The angular power spectrum can then be related to the ensemble average of the $a_{\ell m}$ as

$$\langle a_{\ell m} a_{\ell' m'}^* \rangle = C_\ell^{\Theta\Theta} \delta_{\ell\ell'} \delta_{mm'}. \tag{4.15}$$

The angular power spectrum can be expressed in terms of the initial power spectrum and linear transfer functions [9, 10]. At lowest order in the flat-sky expansion, the angular power spectrum of the CMB anisotropies takes the form [76]

$$C_\ell^{\Theta\Theta} = \frac{1}{2\pi} \int dr dr' dk_\parallel w^{(1)}(\mathbf{k}, r) w^{\star(1)}(\mathbf{k}, r') e^{-ik_\parallel(r-r')} \frac{P_\Phi(k)}{[(r+r')/2]^2} \tag{4.16}$$

where $r = \eta_0 - \eta$, $k_\perp \equiv (\ell + 1/2)/r$ and $k^2 = k_\parallel^2 + k_\perp^2$, and where a star denotes the complex conjugate. If we neglect the integrated effects which occur at low z and affect only the largest scales, we can then approximate that all the signal in $w(\mathbf{k}, \eta)$ arises from the last scattering surface whose thickness is defined from the visibility function $\bar{g}(\eta) \equiv -\bar{\tau}' \exp(-\bar{\tau})$. This visiblity function peaks at r_{LSS} which defines the center of the last scattering surface. In this thin shell approximation, we thus obtain that

$$C_\ell^{\Theta\Theta} \simeq \frac{1}{2\pi} \int dk_\parallel \left| \int dr\, w^{(1)}(\mathbf{k}, r) e^{-ik_\parallel r} \right|^2 \frac{P_\Phi(k)}{r_{\mathrm{LSS}}^2} , \tag{4.17}$$

now with $k_\perp = (\ell + 1/2)/r_{\mathrm{LSS}}$. Additionally, since modes of different m are in general not statistically correlated¶, the phases in the spherical harmonics of (4.6) are unimportant and we can take for practical purposes

$$Q_\ell^m(\hat{\mathbf{k}}) \equiv (-\mathrm{i})^\ell \sqrt{\frac{(\ell - m)!}{(\ell + m)!}} P_\ell^m\left(k_\parallel/k\right) , \tag{4.18}$$

where P_ℓ^m are the associated Legendre polynomials.

4.5. Bispectrum

In a similar way as the angular spectrum, one defines the bispectrum which, again under the assumption of isotropy, is related to the 3-point function of the $a_{\ell m}$ by

$$\langle a_{\ell_1 m_1} a_{\ell_2 m_2} a_{\ell_3 m_3} \rangle = B_{\ell_1 \ell_2 \ell_3}^{\Theta\Theta\Theta} \begin{pmatrix} \ell_1 & \ell_2 & \ell_3 \\ m_1 & m_2 & m_3 \end{pmatrix}, \tag{4.19}$$

where the matrix denotes a Wigner-$3j$ symbol and $B_{\ell_1 \ell_2 \ell_3}^{\Theta\Theta\Theta}$ is the bispectrum. It has become more usual to use the reduced bispectrum $b_{\ell_1 \ell_2 \ell_3}^{\Theta\Theta\Theta}$ [16, 30] which is defined from the bispectrum $B_{\ell_1 \ell_2 \ell_3}^{\Theta\Theta\Theta}$ by

$$B_{\ell_1 \ell_2 \ell_3}^{\Theta\Theta\Theta} \equiv \begin{pmatrix} \ell_1 & \ell_2 & \ell_3 \\ 0 & 0 & 0 \end{pmatrix} \sqrt{\frac{(2\ell_1 + 1)(2\ell_3 + 1)(2\ell_3 + 1)}{4\pi}} b_{\ell_1 \ell_2 \ell_3}^{\Theta\Theta\Theta} . \tag{4.20}$$

In the flat-sky approximation [76], it takes the form

$$b_{\ell_1 \ell_2 \ell_3}^{\Theta\Theta\Theta} = \frac{1}{2\pi} \int dk_{1\parallel} dk_{2\parallel} dr_1 dr_2 dr_3 e^{-ik_{1\parallel}(r_1 - r_3)} e^{-ik_{2\parallel}(r_2 - r_3)} \tag{4.21}$$

$$\times w^{(1)}(\mathbf{k}_1, r_1) w^{(1)}(\mathbf{k}_2, r_2) w_{\mathrm{NL}}^{\star(2)}(\mathbf{k}_1, \mathbf{k}_2, r_3) \frac{P_\Phi(k_1)}{r_1^2} \frac{P_\Phi(k_2)}{r_2^2} + 2 \text{ sym.} ,$$
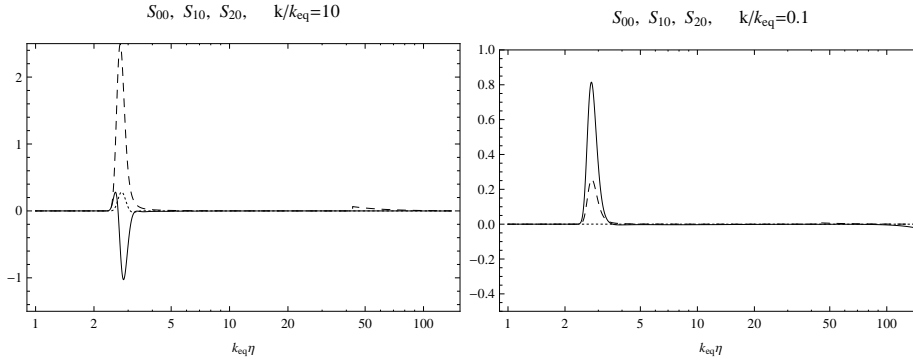
where

$$k_{1\perp} \equiv \ell_1/r_1 , \quad k_{2\perp} \equiv \ell_2/r_2 , \tag{4.22a}$$

$$\frac{k_{3\perp}}{r_3} \equiv \frac{\ell_3^2}{r_1 r_2} + \frac{\ell_1^2}{r_1 r_2}\left(\frac{r_2}{r_1} - 1\right) + \frac{\ell_2^2}{r_1 r_2}\left(\frac{r_1}{r_2} - 1\right) . \tag{4.22b}$$

¶ Note that in our case this is also the case because we consider scalar modes at first order in the perturbations.

We also remind that, since $\mathbf{k}_3 = \mathbf{k}_1 + \mathbf{k}_2$, the parallel components are related according to $k_{3\parallel} = k_{1\parallel} + k_{2\parallel}$. Similarly to the spectrum, this expression can be avantageously simplified in the case where the emitting sources peak in a narrow range of distances. More precisely, provided that the first order emitting sources are peaked in a narrow range of distance, which is the case if we neglect the late ISW effect, the following approximation holds out of the largest scales. In order to grasp how sharply peaked the first order emitting sources are, we plot them in Fig. 1 for $\ell = 0, 1, 2$ for scalar perturbations ($m = 0$). In this thin shell approximation, the expression (4.21) can be

Figure 1. First order scalar emitting sources S_ℓ^0 with $\ell = 0, 1, 2$ in respectively solid, dashed and dotted lines. The plot on the left corresponds to a mode which is well inside the Hubble radius around recombination time, whereas the plot on the right corresponds to a mode which is still super-Hubble around recombination time. In both cases the contributions are sharply peaked and this defines the last-scattering surface and validates the flat-sky approximation.

simplified to give

$$
b_{\ell_1\ell_2\ell_3}^{\Theta\Theta\Theta} = \frac{1}{2\pi} \int \mathrm{d}k_{1\parallel}\mathrm{d}k_{2\parallel} \left[\left(\int \mathrm{d}r_1 w^{(1)}(\mathbf{k}_1, r_1) e^{-\mathrm{i}k_{1\parallel}r_1} \right) \left(\int \mathrm{d}r_2 w^{(1)}(\mathbf{k}_2, r_2) e^{-\mathrm{i}k_{2\parallel}r_2} \right) \right.
$$
$$
\left. \times \left(\int \mathrm{d}r_3 e^{\mathrm{i}(k_{1\parallel}+k_{2\parallel})r_3} w_{\mathrm{NL}}^{\star(2)}(\mathbf{k}_1, \mathbf{k}_2, r_3) \right) \right] \frac{P_\Phi(k_1)P_\Phi(k_2)}{r_{\mathrm{LSS}}^4} + 2 \text{ perm.} \quad (4.23)
$$

now with the simpler flat-sky relations

$$
k_{1\perp} \equiv \ell_1/r_{\mathrm{LSS}}, \quad k_{2\perp} \equiv \ell_2/r_{\mathrm{LSS}}, \quad k_{3\perp} \equiv \ell_3/r_{\mathrm{LSS}}. \quad (4.24)
$$

From the rotational invariance of the spectrum, we can also use the expression (4.18) in the computation of $w^{(1)}$ and $w^{(2)}$. Furthermore, given the definition of the multipoles with the factor N_ℓ [53], the symmetries $k_{1\parallel} \to -k_{1\parallel}$ and $k_{2\parallel} \to -k_{2\parallel}$ correspond to $\alpha \to \pi - \alpha$, and since $b_{\ell_1\ell_2\ell_3}^{\Theta\Theta\Theta}$ is real, we can replace $\exp[\mathrm{i}m\alpha(\mathbf{k}_1, \mathbf{k}_2)]$ by $\cos[m\alpha(\mathbf{k}_1, \mathbf{k}_2)]$ in Eq. (4.12).

5. Numerical implementation

5.1. Width of correlations

In the expression (4.16) of the spectrum, the term multiplying $\mathrm{e}^{-\mathrm{i}k_{\parallel}(r-r')}$ is an almost constant in the regime $k_{\parallel} \ll k_{\perp}$ and is damped, at least by the power spectrum $P_\Phi\left(\sqrt{k_\parallel^2 + k_\perp^2}\right)$, when $k_{\parallel} \gg k_{\perp}$. It follows that the integration over $k_{\parallel}$ leads to a

window function [40] of argument $(r - r')$ whose width is of the order $1/k_\perp \simeq r_{\text{LSS}}/\ell$. A similar argument holds for the bispectrum and the integration over $k_{1\parallel}$ and $k_{2\parallel}$ in Eq. (4.21) leads to two window functions, one for $(r_1 - r_3)$ with a typical width $1/k_{1\perp} \simeq r_{\text{LSS}}/\ell_1$, and a second for $(r_2 - r_3)$ with a typical width $1/k_{2\perp} \simeq r_{\text{LSS}}/\ell_2$. We thus conclude that for a given mode ℓ, the typical scale of correlation is given by r_{LSS}/ℓ. This justifies why we can safely split the effects between primary and secondary effects, that is between early and late time effects. Indeed, at first order, the gravitational potential reaches a constant value until the Universe starts to be dominated by the cosmological constant. The integrated effects are then separated into an early effect, that is before the potential freezes, and a late effect when it starts evolving again. Since the correlations of physical effects must occur at approximately the same distance, then even if integrated effects occur everywhere at second order as the potential grows, they would only contribute in the CMB bispectrum by correlation with the first order early and late effects. As a result, when we are interested in the bispectrum, the second order effects can still be split into primary and secondary effects. In the numerical implementation of Eq. (4.21), this implies that, as long as we neglect the late ISW, we only need to integrate over r_3 in a range of r_{LSS} plus or minus a few times r_{LSS}/ℓ to encompass the early ISW.

5.2. Numerical integration

The numerical integration can be sketched as follows.

(I) We first integrate numerically the sources. Using the initial conditions defined in § 3, we integrate numerically in Fourier space the coupled system constituted of (1) the Einstein equation, (2) the Boltzmann equation both up to second order in the perturbations and (3) the recombination equation up to first order in the perturbations. We first need to integrate the first order equations and then use their results to determine the sources of the second order integration.

(II) We then compute the line of sight expressions (4.17) and (4.23) respectively for the spectrum and for the bispectrum, with their flat sky approximation.

Let us emphasize the following details:

- All our numerics assume the cosmological parameters as determined by WMAP-5 [60].

- The numerics requires to sample the Fourier space and for each Fourier configuration to integrate numerically in time. At first order, we only need to sample the norm k of the mode $\mathbf{k}$, since we aligned the mode with the azimuthal direction. At second order, we also align $\mathbf{k}$ with the azimuthal direction. We only need to sample k_1 and k_2 and the cosinus of the angle (μ_{12}) between $\mathbf{k}_1$ and $\mathbf{k}_2$.

- The Boltzmann hierarchy has to be truncated in order to avoid spurious reflections. We use the closing relations defined in Ref. [70] for both the first and the second order. The latter being defined only for scalar modes, we need to supplement them with the appropriate closing relations for the modes with $m \geq 1$ that appear at the second order. These can be found in Ref. [79] and we report them as well in Appendix D.

- We use $\ell_{\max} = 8$ at first order and $\ell_{\max} = 5$ at second order for the truncation of the Boltzmann hierarchy.

- The line of sight integrals for the spectrum and for the bispectrum are then sampled only up to 3 times the caracteristic scale of the correlation (i.e. r_{LSS}/ℓ) from the end of the last scattering surface.

- We do not include the late ISW and our results hold only for $\ell \gtrsim 10$.

- The code used runs in *Mathematica* and is freely available with documentation on the webpage [58]. The package `CMBquick1` contains all the functions used for the first order integrations including the transfer functions and the spectra, while the package `CMBquick2` contains in the same way all the functions used in the second order integrations.

5.3. Transfer functions
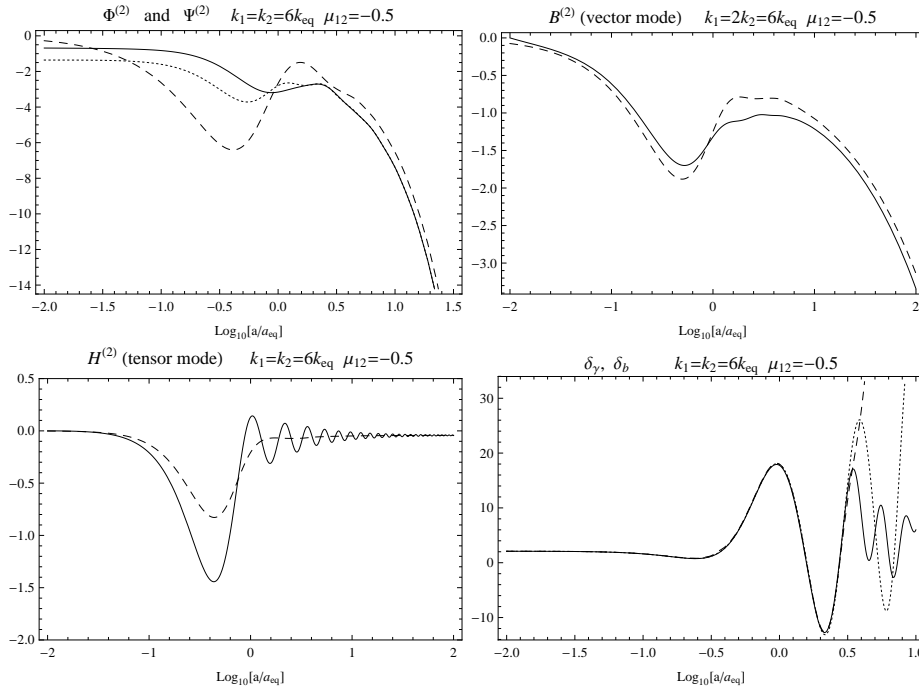
Figure 2. Top left: $\Phi^{(2)}$ and $\Psi^{(2)}$ are in plotted in solid and dotted lines respectively. Top right: Vector perturbation $B^{(2)}$ (solid line); Bottom left: Tensor perturbation $H^{(2)}$ (solid line). For all these panels, the asymptotic transfer functions in the limit $a/a_{\mathrm{eq}} \gg 1$ are depicted in dashed line. Bottom right: Second order energy density contrasts for the radiation, δ_γ (solid), and baryons; δ_b (long dashed). The tight coupling approximation which holds as long as $\tau'/k \gg 1$, is drawn in dotted line.

Fig. 2 depicts the transfer functions at second order, using a definition similar to Eq. (4.11), for the scalar, vector and tensor degrees of freedom of the metric, restricting to the particular configuration $k_1 = k_2 = 6k_{\mathrm{eq}}$ and $\mu_{12} = -0.5$. These transfer functions, computed numerically and without any approximation are perfectly compatible with the ones reported in Ref. [49] obtained from an approximation of the Boltzmann equation. This gives an a posteriori confirmation of the physical

understanding we have provided in Ref. [49] and we refer to this article for further discussion.

Fig. 2 also compares the transfer functions to their asymptotic behaviours in the limit $a/a_{\rm eq} \gg 1$. These asymptotic behaviours correspond to the transfer functions computed in a purely matter dominated universe, and we have checked that they match with their previous estimations [40].

Note that the vector modes transfer function almost vanishes when $k_1 = k_2$ for all μ_{12} since in that case the only contribution arises from the coupling of the anisotropic stress contracted with gradients [80]. Indeed in the harmonic decomposition of terms like $X\partial_I Y$, the terms for $m = 1$ and $m = -1$ vanish for symmetry reasons when $k_1 = k_2$. For such configurations, the contributions to vector production then arise solely from terms of the form $X^{ij}\partial_J Y$. As a consequence, we have plotted a Fourier configuration which escapes this restriction.

5.4. Reduced bispectra

5.4.1. Relation between bispectra In § 4.1, we emphasized the different possible definitions of temperature. Each definition defines a bispectrum while it does not affect the spectrum.

While the most straightforward would be to use the bispectrum of the temperature brightness Θ defined in Eq. (4.1), the previous literature [38] has focused on the bispectrum of the bolometric temperature T defined in Eq. (4.2). And, as we emphasized, to avoid the spectral distortion that affect the bolometric temperature, it may be more robust to use the occupation number temperature T_N. Let us now discuss the relation between the bispectra of these 3 quantities.

First, it is obvious from Eqs. (4.1) and (4.2) that

$$b_{\ell_1\ell_2\ell_3}^{TTT} = b_{\ell_1\ell_2\ell_3}^{T_{\mathcal{I}}T_{\mathcal{I}}T_{\mathcal{I}}} - 3\left(C_{\ell_1}C_{\ell_2} + C_{\ell_2}C_{\ell_3} + C_{\ell_1}C_{\ell_3}\right). \tag{5.1}$$

Then, we deduce from Eq. (4.3) that the total second order information is carried by the combinattion of $b_{\ell_1\ell_2\ell_3}^{T_{\rm N}T_{\rm N}T_{\rm N}}$ and $b_{\ell_1\ell_2\ell_3}^{yT_{\rm N}T_{\rm N}}$. It follows that

$$b_{\ell_1\ell_2\ell_3}^{T_{\rm N}T_{\rm N}T_{\rm N}} = b_{\ell_1\ell_2\ell_3}^{TTT} - b_{\ell_1\ell_2\ell_3}^{yT_{\rm N}T_{\rm N}} - b_{\ell_2\ell_3\ell_1}^{yT_{\rm N}T_{\rm N}} - b_{\ell_3\ell_1\ell_2}^{yT_{\rm N}T_{\rm N}}. \tag{5.2}$$

In conclusion, it is an easy translation to switch from one bispectrum to the other (once the evolution of y is known but this has been achieved in Ref. [57]). In order for our results to be easily compared to the previous literature, we will only consider the bolometric temperature.

5.4.2. Examples of numerical results Representing the bispectrum completely would require a four dimensional plot. For the sake of clarity, we restrict our presentation to few specific configurations. But once again any other configuration is accessible via the use of the packages made available in [58]. On Fig. 3, we show the explicit shape of the bispectrum that we have found and show the three contributions coming from the sources with $m = 0$, $m = 1$ and $m = 2$ respectively[+]. We see that the scalar

---

[+] Note that the meaning of ℓ for a source term is indeed ambiguous since for instance if we consider the gradient of a scalar, it contributes in the source with $\ell = 1$ and $m = 0$ in an integrated effect. However if we perform an integration by part of the form $\partial_I X = {\rm d}X/{\rm d}\eta - \partial X/\partial\eta$ then the total derivative contributes in the source term $\ell = m = 0$ in an effect on the last scattering surface, and the partial derivative contributes as well in $\ell = m = 0$ in an integrated effect. Actually, at first order, this is precisely what happens to the term $\partial_I \Phi^{(1)}$ and that is why after an integration by parts it contributes to the Sachs-Wolfe effect and as an integrated effect. Furthermore, there is no

contribution, that is from sources with $m = 0$ is dominant, especially on small scales. The top panel corresponds to equilateral configurations (with a varying size) and the bottom panels to squeezed cases (isosceles triangles) with length ratio of 10 for the middle panel and a fixed value $l_1 = 20$ for the bottom. The curves are given as a function of l_3.

6. Implications for the detection of the bispectrum

The previous sections have allowed us to numerically compute different bispectra taking into account the full non-linear evolution of the cosmological perturbations and compare it to different types of primordial non-Gaussianities. We now turn, in § 6.1 to the question of defining an equivalent $f_{\rm NL}$ and then to the estimation of the signal to noise ratio in § 6.2.

6.1. Equivalent $f_{\rm NL}$

We follow the extensive previous works [25, 35, 38, 39, 40, 71] in order to define what is the equivalent $f_{\rm NL}$, noted $\widehat{f}_{\rm NL}$, that the primary non-linear effects would induce.

More precisely, let us consider an ideal experiment, that would be only cosmic variance limited, and a statistical estimator designed to detect the primordial non-Gaussianity of the type $f_{\rm NL}^{\Phi}$ assuming a linear evolution of the cosmological fields. Then $\widehat{f}_{\rm NL}$ is precisely what such an estimator would actually measure because of the non-linear dynamics. In summary, for a given choice of model for the primordial couplings, $f_{\rm NL}^{\Phi}$ is such that
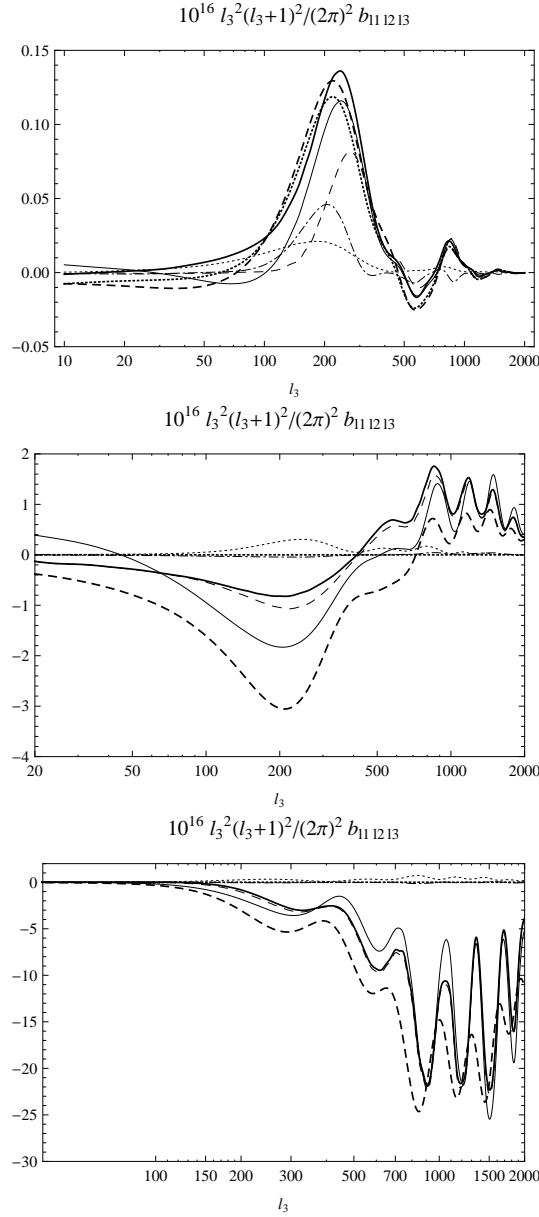
$$\text{Signal} \begin{pmatrix} f_{\rm NL}^{\Phi} = \widehat{f}_{\rm NL} \\ \text{with} \\ \text{linear evolution} \end{pmatrix} = \text{Signal} \begin{pmatrix} f_{\rm NL}^{\mathcal{R}_M} = 0 \\ \text{with} \\ \text{non-linear evolution} \end{pmatrix}. \tag{6.1}$$

According to this point of view, the signal coming from the second order evolution represents a spurious signal, a noise, and $\widehat{f}_{\rm NL}$ is the amplitude of that noise. Of course from an observational point of view, this is not a genuine noise and is not related to any experimental imperfections. It may also have some interests on its own! In the future, it will have to be incorporated consistently in the design of the estimators of primordial non-Gaussianity.

Being mostly interested in the equilateral and the local configurations, we report in Fig. 4 $\widehat{f}_{\rm NL}$ for these two configurations as a function of the maximum multipole $\ell_{\max}$ used.

We have also plotted on Fig. 4 the $\widehat{f}_{\rm NL}$ arising only from the scalar $(m = 0)$ purely second order source. As expected from our previous analysis [49] and from the numerical results of the previous section, these are clearly the dominant contributions. When comparing with the $\widehat{f}_{\rm NL}$ coming from the secondary non-linear effects as reported in Ref. [39], we observe that the primary effects are of slighlty less importance for the local case while they are far more important for the equilateral case. For the local

physical meaning in splitting the contributions of the sources into purely second order terms and quadratic terms as in Ref. [38] since this decomposition is not gauge invariant. Additionally, there can be large contributions of opposite sign which thus nearly cancel as for instance on large scales (see § 7.3 or Refs. [32, 40]) so that picking up a single contribution may be misleading and give an overestimation of the signal. With the same argument, the coupling of the first order collision term with the perturbed ionization fraction which has been studied in Refs. [36, 37, 81] is also not a gauge invariant quantity and we do not try to reproduce these results for this reason.

$$10^{16}\, l_3^{\,2}(l_3+1)^2/(2\pi)^2\, b_{l1\,l2\,l3}$$

$$10^{16}\, l_3^{\,2}(l_3+1)^2/(2\pi)^2\, b_{l1\,l2\,l3}$$

$$10^{16}\, l_3^{\,2}(l_3+1)^2/(2\pi)^2\, b_{l1\,l2\,l3}$$

Figure 3. Comparison of the bispectrum induced by the non-linear dynamics (thick solid line) to a primordial bispectrum with $f_{\rm NL}^{\Phi} = 5$ (thick dashed line for local type, thick dotted line for the equilateral type). We also plot the approximation of Ref. [49] that is considering only purely second order scalar sources in thin solid line, and the contribution from sources for $m = 0, 1, 2$ in respectively thin dashed, dotted, and dot-dashed lines. We considered three different configurations in ℓ space, from top to bottom: an equilateral configuration with $\ell_1 = \ell_2 = \ell_3$ and then two squeezed configurations with $10\ell_1 = \ell_2 = \ell_3$ and $\ell_1 = 20$ with $\ell_2 = \ell_3$.
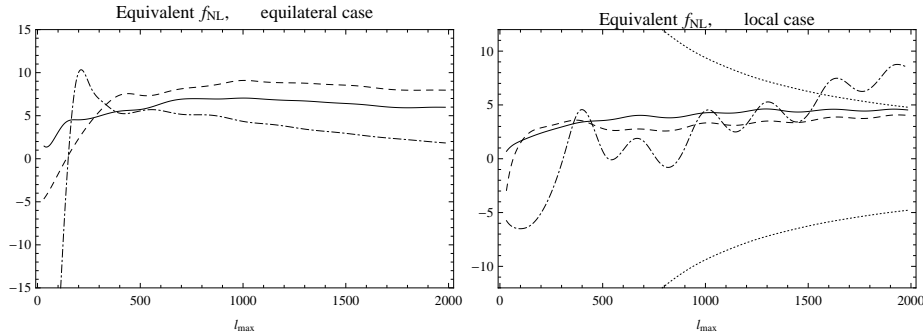
Figure 4. Comparison of $\widehat{f}_{\mathrm{NL}}$ (solid line) induced by the non-linear dynamics to $\widehat{f}_{\mathrm{NL}}$ obtained by including only the scalar ($m = 0$) modes (dashed line) of the purely second order sources, which corresponds to the approximation of our previous work [49]. We also plot $\widehat{f}_{\mathrm{NL}}$ (dot-dashed lined) induced by lensing-ISW secondary effect. Right panel corresponds to local type couplings and the left panel to equilateral type couplings and the $\pm\sigma$ detection limit of f_{NL}^{Φ} is depicted in dotted lines for the local type couplings case.

case, the contributions to $\widehat{f}_{\mathrm{NL}}$ from primary and secondary effects have the same sign. The sum of the primary and secondary effects is then beyond the 2σ limit of detection when $\ell_{\max} > 1500$. This is certainly above the detection limit of *Planck* since it uses multipoles up to $\ell_{\max} \simeq 2000$ and it should thus be taken into account. The primary effects alone would bias the measurement of the local type non-Gaussianity by $\Delta f_{\mathrm{NL}}^{\Phi} \simeq 5$.
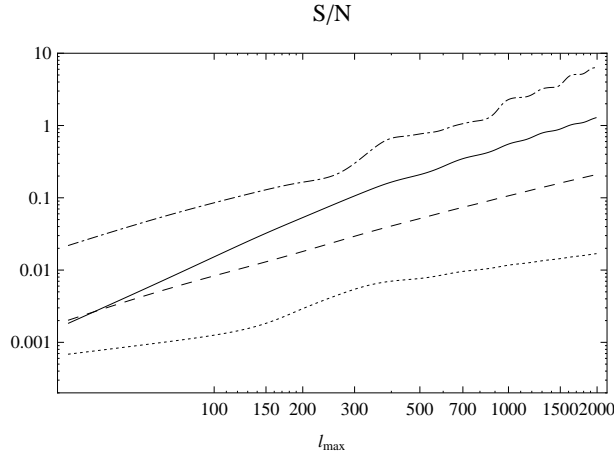
6.2. Signal to noise

We can now report the signal to noise ratio (S/N) as a function of the maximum multipole $\ell_{\max}$ used in the estimator described in Refs. [39, 82]. Fig. 5 represents the signal to noise ratio of the primordial bispectra, both for the local and equilateral cases, as well as the signal to noise ratio of the bispectrum generated by non-linear effects. We also superimpose the signal to noise ratio of the bispectrum generated by ISW-lensing correlations (see § 7.2). We found that the signal to noise ratio of the bispectrum generated by the non-linear dynamics reaches unity for $\ell_{\max} = 2000$.

7. Analytical understanding of the limiting cases

The aim of the section is to derive analytical formulae, a priori valid in asymptotic regimes, that offer theoretical insights on the underlying physics. We first ignore the contribution of neutrinos, and thus set $f_{\mathrm{r}} = 1$, since they play only a marginal role it will greatly simplify the expressions obtained.

After rewriting the Boltzmann equation in § 7.1, we first focus on secondary anisotropies in § 7.2. We then consider the large angular scale limit in § 7.3 (considering separately local and equilateral configurations) separately and then the small angular scale limit in § 7.4.

S/N

Figure 5. The signal to noise ratio as a function of the maximum multipole $\ell_{\max}$ for an ideal experiment. The signal to noise ratio of the total bispectrum generated by non-linear effects (solid line), of the local type primordial bispectrum (dashed line) and of the equilateral type (dotted line) when $f_{\mathrm{NL}}^{\Phi} = 1$. We also plot the signal to noise ratio of the bispectrum due to the ISW-lensing correlation in dot-dashed line.

7.1. Rewriting the Boltzmann equation non perturbatively

Since the Boltzmann equation is solved numerically by using the line of sight approach, it is convenient to rewrite it in terms of the total time derivative along geodesics. It has been noted that defining

$$\exp[2\Phi_{\mathrm{BRM}}] \equiv 1 + 2\Phi\,, \qquad \exp[-2\Psi_{\mathrm{BRM}}] \equiv 1 - 2\Psi\,, \tag{7.1}$$

simplifies its expression [83]. In particular, the Boltzmann equation, written non perturbatively (that is in such a way that it is valid up to any order in perturbations), can be recast as

$$e^{\bar{\tau}} \frac{\mathrm{d}\left(e^{-\bar{\tau}}\tilde{\mathcal{I}}\right)}{\mathrm{d}\eta} + \frac{\partial\tilde{\mathcal{I}}}{\partial n^i}\frac{\mathrm{d}n^i}{\mathrm{d}\eta} - 4\frac{\tilde{\mathcal{I}}}{E}\frac{\mathrm{d}E}{\mathrm{d}\eta} = e^{\Phi_{\mathrm{BRM}}}\mathcal{C}[\tilde{\mathcal{I}}] + \bar{\tau}'\tilde{\mathcal{I}}\,. \tag{7.2}$$

In this expression, E stands for the scale factor multiplied by the energy[*] of a photon[♯], $\tilde{\mathcal{I}}(\mathbf{x}, \eta, n^i)$ is the reduced brightness of the radiation, that is the brightness divided by its average value (this implies that $\bar{\tilde{\mathcal{I}}} = \bar{\tilde{\mathcal{I}}}_0^0 = 1$). Note also that $\mathrm{d}/\mathrm{d}\eta$ is the total derivative on the perturbed space-time which includes the convective derivative, but not lensing, i.e. defined on the perturbed space-time by

$$\frac{\mathrm{d}}{\mathrm{d}\eta} \equiv \frac{\partial}{\partial\eta} + \frac{\partial x^I}{\partial\eta}\frac{\partial}{\partial x^I}\,. \tag{7.3}$$

While being very general, E cannot be specified so easily in a non perturbation manner, and neither can we obtain a non perturbative expression of the collision term. However, up to second order we obtain

$$\frac{1}{E}\frac{\mathrm{d}E}{\mathrm{d}\eta} = -\left[\frac{\mathrm{d}\Phi_{\mathrm{BRM}}}{\mathrm{d}\eta} - \Phi_{\mathrm{BRM}}' - \Psi_{\mathrm{BRM}}' + (H_{IJ}' - \partial_I B_J)\,n^i n^j\right]\,, \tag{7.4}$$

[*] In Ref. [53] E is noted ap^o and in Ref. [35] it is noted ap. Since this is the energy of photons, we use this more obvious notation.

[♯] See Ref. [53] for details about the observer which actually measures this energy.

where we must bear in mind that the vector and tensor modes are only second order quantities. As for the collision term, it is reported in Appendix A.2 up to second order as well.

However, we can go a few steps further in our non-perturbative reformulation of the Boltzmann equation. Indeed, we can integrate by parts $\tilde{\mathcal{I}}\mathrm{d}(\ln E)/\mathrm{d}\eta$, and use the Boltzmann equation itself to replace $(\ln E)\mathrm{d}\tilde{\mathcal{I}}/\mathrm{d}\eta$. We then use that $(\ln E)\mathrm{d}(\ln E)/\mathrm{d}\eta = 1/2\mathrm{d}(\ln E)^2/\mathrm{d}\eta$ and iterate this method and finally resum all the terms to obtain

$$e^{\bar{\tau}}\frac{\mathrm{d}\left[e^{-\bar{\tau}}\tilde{\mathcal{I}}E^{-4}\right]}{\mathrm{d}\eta} + E^{-4}\frac{\partial\tilde{\mathcal{I}}}{\partial n^i}\frac{\mathrm{d}n^i}{\mathrm{d}\eta} = E^{-4}\left[e^{\Phi_{\mathrm{BRM}}}\mathcal{C}[\tilde{\mathcal{I}}] + \bar{\tau}'\tilde{\mathcal{I}}\right] . \qquad (7.5)$$

If we expand the photon geodesic equation in perturbations according to

$$\frac{\partial x^I}{\partial\eta} = \overline{\frac{\partial x^I}{\partial\eta}} + \delta\left(\frac{\partial x^I}{\partial\eta}\right) , \qquad (7.6)$$

we can expand accordingly the total derivative as

$$\frac{\mathrm{d}}{\mathrm{d}\eta} = \overline{\frac{\mathrm{d}}{\mathrm{d}\eta}} + \delta\left(\frac{\mathrm{d}}{\mathrm{d}\eta}\right) , \quad \overline{\frac{\mathrm{d}}{\mathrm{d}\eta}} \equiv \frac{\partial}{\partial\eta} + \overline{\frac{\partial x^I}{\partial\eta}}\frac{\partial}{\partial x^I} . \qquad (7.7)$$

An integral solution of Eq. (7.4) can be found immediatly by integrating the Boltzmann equation over the background geodesics. We obtain finally that the observed brightness today in the direction of observation $-n^i$ is

$$E^{-4}(\eta_0)\tilde{\mathcal{I}}(\eta_0, -n^i) = \int^{\eta_0}\mathrm{d}\eta'\bar{g}(\eta')E^{-4}\left(\mathcal{C}[\tilde{\mathcal{I}}]\frac{e^{\Phi_{\mathrm{BRM}}}}{\bar{\tau}'} + \tilde{\mathcal{I}}\right) - \int^{\eta_0}e^{-\bar{\tau}}E^{-4}\frac{\partial\tilde{\mathcal{I}}}{\partial n^i}\frac{\mathrm{d}n^i}{\mathrm{d}\eta}$$

$$-\int^{\eta_0}e^{-\bar{\tau}}\delta\left(\frac{\partial x^I}{\partial\eta}\right)\partial_I\left(\tilde{\mathcal{I}}E^{-4}\right)\mathrm{d}\eta' . \qquad (7.8)$$

This expression is valid up to any order in the perturbations, but the difficulties are hidden in the computation of E and in the expression of the collision term $\mathcal{C}[\tilde{\mathcal{I}}]$. The first integral on the right hand side encodes the intrinsic anisotropy. As expected, it is weighted by the visibility function and adds up the contributions from the last scattering surface. The second integral contains the lensing effect while the last one is the time delay. This latter contribution has already been computed [82] for the spectrum and for the bispectrum, and its effect is by far negligible for geometric reasons. However, the lensing effect is both a primary effect and a secondary effect since it contributes from the last scattering surface up to now. Since $\mathrm{d}n^i/\mathrm{d}\eta$ vanishes at the background level, we can use the general integral equation (7.8) to express it in terms of the intrinsic anisotropies by iteration. We detail in the next section how this gives rise to a bispectrum when coupled to secondary linear effects.

7.2. Secondary effects

After having reached a constant value in the matter dominated era, the first order potentials remain constant until the cosmological constant eventually starts to dominate the matter content of the Universe. This gives rise to a late integrated effect (which enters in E) known as late Integrated Sachs-Wolfe effect (late ISW). Given the arguments of § 5.1 on the width of the correlation in the bispectrum, the intrinsic second order anisotropy will not correlate to the late ISW. However the lensing term can correlate to the late ISW since it is also an integrated effect. The lensing term is at

least a second order term, and if we make use of the first order Boltzmann equation to replace for $\partial \tilde{\mathcal{I}}^{(1)}/\partial n^i$, it can be recast in (see next section as well as Refs. [82, 84, 85])

$$\nabla^{n^i} \phi^{(1)} \nabla_{n^i} \tilde{\mathcal{I}}(\eta_0, -n^i) \,, \tag{7.9}$$

where $\phi^{(1)}$ is the lensing potential whose expression we give further in Eq. (7.18). Note that in order to obtain this expression, we have to neglect the lensing inside the last scattering surface as well as the lensing of the late ISW. Both approximations are justified from the geometrical properties of the lensing effect since it vanishes when the lens is either at the source or at the observer position. Under these approximations, the lensing term is separable into a lensing term $\phi^{(1)}$ and a lensed term $\mathcal{I}^{(1)}$. The computation of separable terms is straightforward since the lensing potential correlates with the late ISW effect and the lensed source correlates with the temperature emitted on the last scattering surface. Strictly speaking the bispectrum arising from the lensing term is thus a combination of primary and secondary effects††. The reduced bispectrum obtained is given for instance in Refs. [29, 39, 41, 82, 84, 85, 86] and reads

$$b_{\ell_1 \ell_2 \ell_3} = \frac{1}{2} \left[\ell_2(\ell_2+1) + \ell_3(\ell_3+1) - \ell_1(\ell_1+1)\right] C_{\ell_2}^{\phi\Theta_{\text{ISW}}} C_{\ell_3}^{\Theta\Theta} + 5 \text{ sym.}, \tag{7.10}$$

where the prefactor comes from the angular gradients on $\phi^{(1)}$ and $\mathcal{I}^{(1)}$. This method to derive the correlation of the lensing term with first-order secondary effects is general [86, 29]. Reionization for instance will create a late Doppler effect, and the effect of the non-linear structures formation (Rees-Sciama, Sunyaev-Zel'dovich...) can also be mapped to additional secondary linear effects (in an effective manner) in order to apply this method [41, 87] and compute their bispectrum.

7.3. Large scales

7.3.1. Generalities On large scales, that is for modes such that $k\eta_{\text{LSS}} \ll 1$ where η_{LSS} is the average time of recombination, we want to derive the equivalent of the formula $\Theta^{(1)} = \frac{1}{3}\Phi_{\text{LSS}}$ that allows to explain the Sachs-Wolfe plateau of the angular power spectrum. This was already obtained by following the photons geodesics in Refs. [32, 55, 40].

We assume that the last scattering surface is far in the matter dominated era, that is long after the matter-radiation equivalence. We also ignore the effect of the cosmological constant. The Bardeen potentials $\Phi^{(1)}$ and $\Psi^{(1)}$ have then reached a constant value that we label by LSS. On large scales, this is even true at any order in perturbations. The width of the visibility function can also be neglected on large scales, and we approximate $\bar{g}(\eta)$ by a Dirac distribution centered around η_{LSS}, and $e^{-\bar{\tau}}$ by a step function which is unity for $\eta > \eta_{\text{LSS}}$. We can also neglect the velocity fields, that is the velocity moments v_m of baryons and cold dark matter, and the first moment of radiation and neutrinos, that is $\mathcal{I}_1^m$ and $\mathcal{N}_1^m$ since they are suppressed by $k\eta_{\text{LSS}}$. Higher order moments can also be neglected since they are suppressed by higher powers of $k\eta_{\text{LSS}}$.

A first simplification in Eq. (7.8) lies in the fact that the collision term has no monopole on large scales. We further assume that we can neglect the vector and tensor modes and the integrated terms in the derivative of E given by Eq. (7.4). In that simplified case we have

$$E = e^{-\Phi_{\text{BRM}}} \,. \tag{7.11}$$

†† Pure secondary effects appear only at large scale and are thus less interesting since the cosmic variance limits the information extracted from the observations.

The general solution obtained in Eq. (7.8) then reduces to

$$\tilde{\mathcal{I}}(\eta_0, -n^i)e^{4\Phi_{\mathrm{BRM}}(\eta_0)} = \tilde{\mathcal{I}}(\eta_{\mathrm{LSS}})e^{4\Phi_{\mathrm{BRM}}(\eta_{\mathrm{LSS}})} - \int_{\eta_{\mathrm{LSS}}}^{\eta_0} e^{4\Phi_{\mathrm{BRM}}} \frac{\partial \tilde{\mathcal{I}}}{\partial n^i} \frac{\mathrm{d}n^i}{\mathrm{d}\eta}$$

$$- \int_{\eta_{\mathrm{LSS}}}^{\eta_0} \delta\left(\frac{\partial x^I}{\partial \eta}\right) \partial_I \left(\tilde{\mathcal{I}}e^{4\Phi_{\mathrm{BRM}}}\right) \mathrm{d}\eta', \tag{7.12}$$

which is also valid non perturbatively (that is up to any order in perturbations) provided that the approximations hold. We will discard from now on the last integral coming from the time-delay as it is negligible [82]. Restricting to an expression valid only up to second order, we obtain (restoring the potential Φ)

$$\tilde{\mathcal{I}}(\eta_0, -n^i) = 4\Phi_{\mathrm{LSS}} + \tilde{\mathcal{I}}^0_{0\,\mathrm{LSS}} + 4(\tilde{\mathcal{I}}_{\mathrm{LSS}} + \Phi_{\mathrm{LSS}})\Phi_{\mathrm{LSS}} - \int_{\eta_{\mathrm{LSS}}}^{\eta_0} \frac{\partial \tilde{\mathcal{I}}}{\partial n^i} \frac{\mathrm{d}n^i}{\mathrm{d}\eta} \mathrm{d}\eta'. \tag{7.13}$$

Note that in the previous expression, following standard practice, we have omitted the terms which depend on the observer space-time location as they are not observable.

At first order, we obtain the conservation relation

$$\frac{\mathrm{d}\left(\Theta^{(1)} + \Phi^{(1)}\right)}{\mathrm{d}\eta} = \delta_D^1(\eta - \eta_{\mathrm{LSS}})\left(\Theta^{(1)} + \Phi^{(1)}\right), \tag{7.14}$$

where δ_D^1 is the one-dimensional Dirac distribution. We thus recover the textbook result

$$\Theta^{(1)}(\eta_0, -n^i) = \left[\Theta_0^{0(1)} + \Phi^{(1)}\right](\eta_{\mathrm{LSS}}), \tag{7.15}$$

where we recall that Θ is defined in Eq. (4.1). We also recall that the right hand side is evaluated at η_{LSS} on background geodesics defined by the direction n^i and that we have dropped the potential evaluated today since it is not observable.

At second order, we have

$$\Theta^{(2)}(\eta_0, -n^i) = \Theta_{0\,\mathrm{LSS}}^{0(2)} + \Phi_{\mathrm{LSS}}^{(2)} + 2\left[4\Theta_{\mathrm{LSS}}^{(1)} + \Phi_{\mathrm{LSS}}^{(1)}\right]\Phi_{\mathrm{LSS}}^{(1)}$$

$$- 2\int_{\eta_{\mathrm{LSS}}}^{\eta_0} \frac{\partial \Theta^{(1)}}{\partial n^i} \left(\frac{\mathrm{d}n^i}{\mathrm{d}\eta'}\right)^{(1)} \mathrm{d}\eta'. \tag{7.16}$$

The first line of the right hand side represents the intrinsic anisotropy while the last line contains the lensing effect. Using Eq. (7.14) and the fact that the gravitational potential does not depend on the direction of propagation but only on the space-time coordinates, the lensing term can be recast as

$$- \int_{\eta_{\mathrm{LSS}}}^{\eta_0} \frac{\partial \Theta^{(1)}}{\partial n^i} \left(\frac{\partial n^i}{\partial \eta'}\right)^{(1)} \mathrm{d}\eta' = \nabla^{n^i}\phi^{(1)}\nabla_{n^i}\left(\Theta_{\mathrm{LSS}}^{(1)} + \Phi_{\mathrm{LSS}}^{(1)}\right), \tag{7.17}$$

where we have used the first order expression for $\mathrm{d}n^i/\mathrm{d}\eta$ (given in our notation in Ref. [53]), and where we have defined the lensing potential by

$$\phi^{(1)} \equiv - \int_{\eta_{\mathrm{LSS}}}^{\eta_0} \frac{\left[\Phi^{(1)}(\eta') + \Psi^{(1)}(\eta')\right](\eta' - \eta_{\mathrm{LSS}})}{(\eta_0 - \eta')(\eta_0 - \eta_{\mathrm{LSS}})} \mathrm{d}\eta', \tag{7.18}$$

the geometric factor being simply the usual combination of angular distances in a spatially Euclidean universe.

For adiabatic initial conditions, and assuming that the Universe is completely matter dominated during the recombination, we obtain the following initial conditions for the temperature anisotropies

$$\Theta_{0,\text{LSS}}^{0(1)} = -\frac{2}{3}\Phi_{\text{LSS}}^{(1)}, \tag{7.19a}$$

$$\Theta_{0,\text{LSS}}^{0(2)} = -\frac{2}{3}\Phi_{\text{LSS}}^{(2)} + \frac{28}{9}\Phi_{\text{LSS}}^{(1)}\Phi_{\text{LSS}}^{(1)}, \tag{7.19b}$$

which can be obtained easily [40, 55] using $\tilde{\mathcal{I}}_{\text{LSS}} = \exp\left(-8\Phi_{\text{BRM}}^{\text{LSS}}/3\right)$. Furthermore, we can use that in the matter dominated era the second order gravitational potential is given on large scales by

$$\Phi^{(2)} = 2\Phi^{(1)2} + 2\Delta^{-1}(\partial_I\Phi^{(1)}\partial^I\Phi^{(1)}) - 6\Delta^{-2}\partial^I\partial^J(\partial_I\Phi^{(1)}\partial_J\Phi^{(1)}), \tag{7.20}$$

when $f_{\text{NL}}^{\mathcal{R}} = -1$. This enables us to obtain a complete expression of the second order temperature anisotropies on large scales in the case where the approximations made hold.

7.3.2. Local configuration In the local configuration, the primary non-Gaussianity contributes mostly to squeezed configurations of the bispectrum, that is when one of the modes is much smaller than the other two, for instance if $k_1 \ll k_2$. We are thus interested in the contribution of evolution in that same configuration in the ℓ space in order to assess the contribution of non-linear effects to the total CMB bispectrum. The contributions of the purely second order vector and tensor modes are suppressed by k_1/k_2 and can thus be ignored. The same happens for the integrated effects involving $\Phi^{(2)'}$ and $\Psi^{(2)'}$. The equation (7.16) is thus valid in that case. Furthermore, the lensing term [40, 88] can also be neglected in this large scale limit, and we are thus left with the intrinsic anisotropy. For the local configuration we read from (7.20) that $\Phi^{(2)} = 2\Phi^{(1)2}$, and we thus obtain

$$\Theta^{(1)} = \frac{1}{3}\Phi^{(1)}, \qquad \Theta^{(2)} = \frac{4}{9}\Phi^{(1)2}. \tag{7.21}$$

We recover the results of Ref. [40] for the bolometric temperature T, since the expression obtained reads precisely up to second order

$$(T/\bar{T})^4 \equiv \frac{\mathcal{I}}{\bar{\mathcal{I}}} = (1 + 4\Theta) = \exp[4\Phi^{(1)}/3]. \tag{7.22}$$

Should we need to compute the temperature with a non-vanishing $f_{\text{NL}}^{\mathcal{R}_M}$, that is with $f_{\text{NL}}^{\Phi} \neq -1$, the previous result would be modified by replacement of $\Phi^{(1)}$ by $\Phi^1 - (f_{\text{NL}}^{\Phi} + 1)(\Phi^{(1)2} - \langle\Phi^{(1)2}\rangle)$ and the arguments exposed in Ref. [40] for the interpretation of the result would remain unchanged. Note also that this ideal regime is never reached since the last scattering surface is not deep in the matter dominated era. Since the first and second order potentials undergo a change of value between the radiation dominated era and the matter dominated era, the relation $\Phi^{(2)} = 2\Phi^{(1)2}$ is violated around equivalence and in particular on the last scattering surface. This fact implies that the limit in which Eq. (7.22) was obtained cannot be seen from our numerical results.

7.3.3. Equilateral configuration In the equilateral case, the previous approximations do not hold. Indeed the lensing term and the integrated contributions of the scalar, vector and tensor modes cannot be ignored since terms such as $\Delta^{-1}\partial^i\Phi\partial_i\Phi$ are negligible in the squeezed limit but not in an equilateral configuration. Since these effects do not correlate only at the last scattering surface, a proper numerical integration of the bispectrum expression (4.23) has to be performed. They are computed in details in Ref. [40].

7.4. Small scales

On small scales, another approximation scheme can be used in order to assess the order of magnitude of the evolutionary bispectrum. This has been presented in detail in our previous analysis [49], the validity of which has been confirmed by the numerics of the present work. It relies on the assumption that all modes are on sub-Hubble scales, which holds only for non-squeezed configurations. To summarize, it is based on the fact that any perturbation mode of the cold dark matter starts collapsing as soon as it becomes sub-Hubble. The non-linear gravitational potential is thus predominently shaped by cold dark matter component. The photon-baryon plasma then develops acoustic oscillations, that are imprinted on the last scattering surface, with a forcing term given by the non-linear gravitational potential. The convergence of this approximation onto the complete computation is shown on Fig. 4, and we see that it is responsible for most of signal on small scales. In particular, we conclude that the approximation is good as soon as $\ell > 500$.

8. Conclusion

This article presents a complete investigation of the imprint of the non-linear dynamics on the CMB bispectrum. The calculations were carried with all the matter fields of the standard cosmological ΛCDM model included with three families of massless neutrinos. The numerical calculations make use of a full numerical integration of the coupled system of the second order Boltzmann and Einstein equations for both the photons, with their polarization, and the neutrinos. Furthermore, line of sight integrations include first order effects in the recombination history. The initial conditions correspond to adiabatic initial conditions with a vanishing intrinsic primordial non-Gaussianity (in the context of standard single-field inflation, that implies that a contribution of the order of the slow-roll parameters has been neglected).

The numerical integrations were done with the cosmological parameters of the best fit model derived from the WMAP data [60]. This article is focused on the bispectrum of the temperature anisotropies. We have been forced however to define the temperature we use since second order effects are bound to induce spectral distortions. This effect has been described in details in Ref. [57]. Throughout the article, we adopt the bolometric temperature. We do not expect though that a change of definition for the temperature, like the occupation number temperature, would change significantly the conclusions we have reached. This work also demonstrates that the second order Boltzmann equation can be exactly integrated numerically and be used to produce bispectra. The resulting shape and amplitude of those bispectra is the result of intricate phenomena. It is possible though to obtain theoretical insights into peculiar cases, at small or large scale for instance. Those results confirm in particular that, at small scales, the major mechanism at play is the impact of the gravitational coupling

of the dark matter potential during the matter dominated era as it had been put forward in Ref. [49].

It is obviously difficult to grasp those results in details. In order to be able to compare the amplitude of those effects to primordial couplings, we have defined and computed equivalent $f_{\rm NL}$ parameters, $\widehat{f}_{\rm NL}$. They are defined in such a way that it is the signal a statistical indicator designed to measure primordial $f_{\rm NL}$ would get from the amplitude of the temperature bispectrum. We have found that for both primordial non-Gaussianity of local or equilateral types we have $\widehat{f}_{\rm NL} \simeq 5$ for ℓ above 500. When compared to secondary effects, namely ISW-lensing couplings, primary effects are found to be of comparable amplitude. The former are however more efficient in producing a $\widehat{f}_{\rm NL}$ for the local type ; the situation is reverse for the equilateral type for which the signal comes predominantly from the primary effects.

Evaluations of signal to noise ratio however show that the non-Gaussianity induced by the primary second order effects in the temperature field alone can only be marginally detected by the *Planck* mission. Secondary effects are more likely to be detected. This is however the first ever explicit and complete computation of these effects and even though the concordant model does not offer a good chance of detection, it might be a good way to put constraints on alternative cosmological models.

We remind that the numerical tools used in this article are freely available and can be downloaded at [58] so that many other bispectrum configurations and transfer functions can be investigated at will. The code make uses of a flat sky approximation. It is accurate enough for our purpose and this approximation does not interfere with the resolution of the Boltzmann equation. The code should also be complemented with secondary non-linear effects, that have been investigated in Refs. [39, 41, 86].

Appendix A. Governing equations

Appendix A.1. Einstein equations

We use the standard definition that for a species labelled by a, $\Omega_a \equiv \bar{\rho}_a/(3\mathcal{H}^2)$. When unspecified, a runs on r, ν, b, c that is on photons, neutrinos, baryons and cold dark matter. We also use the definition $\kappa \equiv 8\pi G$. In the expressions of the quadratic sources, it is implicitly meant that the two perturbation variables in each quadratic term are first order variables. We thus omit the order superscript in that case to alleviate the notation. We have a set of four scalar equations (see Refs. [26, 52, 89])

$$\Delta\Psi^{(2)} - 3\mathcal{H}\Psi^{(2)'} - 3\mathcal{H}^2\Phi^{(2)} - \frac{\kappa}{2}\sum_a \rho_a^{(2)} = S_1 \,, \tag{A.1}$$

$$\Psi^{(2)''} + \mathcal{H}^2\Phi^{(2)} + \frac{1}{3}\Delta(\Phi^{(2)} - \Psi^{(2)}) + \mathcal{H}\Phi^{(2)'} + 2\mathcal{H}\Psi^{(2)'}$$
$$+ 2\mathcal{H}'\Phi^{(2)} - \frac{\kappa}{6}\sum_{a=r,\nu} \rho_a^{(2)} = S_2 \,, \tag{A.2}$$

$$\Psi^{(2)} - \Phi^{(2)} + \frac{\kappa}{5}\Delta^{-1}\left(\bar{\rho}_r\mathcal{I}_2^{2(2)} + \bar{\rho}_\nu\mathcal{N}_2^{2(2)}\right) = S_3 \,, \tag{A.3}$$

$$\Psi^{(2)'} + \mathcal{H}\Phi^{(2)} + \frac{\kappa}{2}\sum_a \bar{\rho}_a(1 + w_a)V_a^{(2)} = S_4 \,. \tag{A.4}$$

Their quadratic source terms read respectively

$$S_1 = -8\Psi\Delta\Psi - 3\partial_I\Psi\partial^I\Psi - 3\Psi'^2 + \kappa\sum_a \bar{\rho}_a(1+w_a)\partial_I V_a\partial^I V_a,$$

$$- 12\mathcal{H}(\Phi-\Psi)\Psi' - 12\mathcal{H}^2\Phi^2 \tag{A.5}$$

$$S_2 = 4\mathcal{H}^2\Phi^2 + \frac{8}{3}\Psi\Delta\Psi + 8\mathcal{H}(\Phi-\Psi)\Psi' + 8\mathcal{H}'\Phi^2 - \Psi'^2 + 2\Phi'\Psi'$$

$$+ \frac{2}{3}\partial_I\Phi\partial^I\Phi + \frac{2}{3}\partial_I\Phi\partial^I\Psi + \partial_I\Psi\partial^I\Psi + \frac{\kappa}{3}\sum_a \bar{\rho}_a(1+w_a)\partial_I V_a\partial^I V_a$$

$$+ \frac{4}{3}(\Phi-\Psi)\Delta\Phi + 8\mathcal{H}(\Phi-\Psi)\Psi' + 4(\Phi-\Psi)\Psi'', \tag{A.6}$$

$$S_3 = -4\Psi^2 - 2\Phi^2$$

$$- \Delta^{-1}\left[\partial_I(\Psi+\Psi)\partial^I(\Psi+\Phi) + 2\Psi\Delta\Phi + \sum_a \kappa\bar{\rho}_a(1+w_a)\partial_I V_a\partial^I V_a\right]$$

$$+ 3(\Delta\Delta)^{-1}\partial_I\partial_J\left[\partial^I(\Psi+\Phi)\partial^J(\Psi+\Phi) + 2\Psi\partial_I\partial_J\Phi\right.$$

$$\left. + \kappa\sum_a \bar{\rho}_a(1+w_a)\partial^I V_a\partial^J V_a\right], \tag{A.7}$$

$$S_4 = 2\mathcal{H}\Phi^2 - 4\Psi\Psi' + 2\partial_I^{-1}(\Psi'\partial_I\Psi)$$

$$+ \kappa\sum_a \bar{\rho}_a\partial_I^{-1}\left[(1+w_a)\Psi\partial_I V_a - (1+c_{s,a}^2)\delta_a\partial_I V_a\right]. \tag{A.8}$$

These expressions are easily computed in Fourier space using that [53]

$$[\partial_I V^{(1)}\partial^I V^{(1)}](\mathbf{k}) = -\mathcal{K}\left\{\mathbf{k}_1.\mathbf{k}_2 V^{(1)}(k_1)V^{(1)}(k_2)\right\} \tag{A.9}$$

$$= -\mathcal{K}\left\{\sum_{n=-1}^{1}(-1)^n v_n^{(1)}(\mathbf{k}_1)v_{-n}^{(1)}(\mathbf{k}_2)\right\} \tag{A.10}$$

$$= -\mathcal{K}\left\{\hat{\mathbf{k}}_1.\hat{\mathbf{k}}_2 v_0^{(1)}(k_1)v_0^{(1)}(k_2)\right\} \tag{A.11}$$

since

$$[\partial_I V^{(1)}](\mathbf{k}) = i\hat{k}_I v_0^{(1)}(k), \tag{A.12}$$

$$v_m^{(1)}(\mathbf{k}) = -\hat{k}^{(m)}v_0^{(1)}(k), \tag{A.13}$$

$$\mathbf{k}_1.\mathbf{k}_2 = k_1^I k_{2I} = \sum_{n=-1}^{1}(-1)^n k_1^{(n)}k_2^{(-n)}, \tag{A.14}$$

where $\hat{k}_I \equiv k_I/k$ and $k^2 \equiv k_I k^I$. The notation V denotes here the scalar part of the velocity field in the coordinate frame, whereas the moments v_m are taken in a local Minkowski frame. See Ref. [53] for the precise definitions of these decompositions.

Note also that in order to express terms like

$$3(\Delta\Delta)^{-1}\partial_I\partial_J\left(\partial^I\Phi\partial^J\Phi\right) - \Delta^{-1}\partial_I\Phi\partial^I\Phi, \tag{A.15}$$

in function of the multipolar components of the modes $k_1^{(n)}$ and $k_2^{(-n)}$, we can use the identity (see Appendix A.2 for definitions)

$$\sum_{n=-1}^{1} {}_n\lfloor K_2^0\, k_1^{(n)}k_2^{(-n)} = 3(\hat{\mathbf{k}}.\mathbf{k}_1)(\hat{\mathbf{k}}.\mathbf{k}_2) - \mathbf{k}_1.\mathbf{k}_2. \tag{A.16}$$

As for the second order metric vector modes, we can determine them from the constraint (that we only report here in Fourier space)

$$-\frac{k^2}{2}B_m^{(2)} = \kappa \sum_a \bar{\rho}_a(1+w_a)v_{a,m}^{(2)} + S_{\rm V} \tag{A.17}$$

with

$$S_{\rm V} = \mathcal{K} \left\{ 4\Psi^{(1)'}(k_1)k_2^{(m)}\Phi^{(1)}(k_2) \right. \tag{A.18}$$

$$\left. +2\kappa \sum_a \bar{\rho}_a(1+w_a)\left(\frac{\rho^{(1)}(k_1)}{\bar{\rho}_a} - \Phi^{(1)}(k_1) - \Psi^{(1)}(k_1)\right) v_{a,m}^{(1)}(k_2) \right\} .$$

Finally the second order tensor modes are determined by a second order differential equation which describes how they are sourced by quadratic terms,

$$H_m^{(2)''}(k) + 2\mathcal{H}H_m^{(2)'}(k) + k^2 H_m^{(2)} = \frac{2\kappa}{15}\left(\bar{\rho}_{\rm r}\mathcal{I}_2^{m(2)} + \bar{\rho}_\nu \mathcal{N}_2^{m(2)}\right) \tag{A.19}$$

$$+\,_0^{}\!\!\downarrow\!K_2^2\frac{2}{3}\mathcal{K}\left\{ k_2^{(1)}k_1^{(1)}[\Phi^{(1)}(k_1)\Phi^{(1)}(k_2) + \Psi^{(1)}(k_1)\Psi^{(1)}(k_2)] + \sum_{a={\rm b,c}} \kappa\bar{\rho}_a v_{a,1}^{(1)}(k_1)v_{a,1}^{(1)}(k_2) \right\} .$$

Appendix A.2. Boltzmann equation for radiation

Appendix A.2.1. General remarks As mentionned in § 2.3 (see also Ref. [53]) it is sufficient to specify the purely second order part and the quadratic part of an equation to fully specify it at first and second order. The Boltzmann equation, which is formally written

$$\mathcal{L}[\mathcal{X}] = \mathcal{C}[\mathcal{X}], \tag{A.20}$$

where $\mathcal{X}$ stands for $\mathcal{I}$, $\mathcal{E}$ and $\mathcal{B}$, and where $\mathcal{L}$ and $\mathcal{C}$ are respectively the Liouville operator and the collision operator. We decompose the operators in the form

$$\mathcal{L}[\bar{\mathcal{X}},\mathcal{X}^{(1)},\mathcal{X}^{(2)}] = \bar{\mathcal{L}}[\bar{\mathcal{X}}] + \mathcal{L}^{(1)}[\bar{\mathcal{X}},\mathcal{X}^{(1)}] + \frac{1}{2}\left(\mathcal{L}^{(2)}[\bar{\mathcal{X}},\mathcal{X}^{(2)}] + \mathcal{L}^{(1)(1)}[\bar{\mathcal{X}},\mathcal{X}^{(1)}]\right) ,\tag{A.21}$$

and similarly for $\mathcal{C}$. The details of the derivation with our present notation can be found in Ref. [53] (see also Refs. [83, 90]). Contrary to what has been performed in Ref. [53] we choose to report here the Boltzmann equation in the form $\mathcal{L}[] = \mathcal{C}[]$ rather than in the form $\mathcal{L}^\#[] = \mathcal{C}^\#[]$, in order to facilitate the comparison with existing literature. We will use the following definitions that will simplify the notation

$$_s^0\!\!\uparrow\!K_\ell^m \equiv\,_s^0\!\!\downarrow\!K_\ell^m \equiv \sqrt{\frac{(\ell^2-m^2)(\ell^2-s^2)}{\ell^2}} , \tag{A.22}$$

$$_s^{\pm 1}\!\!\uparrow\!K_\ell^m \equiv -\sqrt{\frac{(\ell\pm m)(\ell\pm m+1)(\ell^2-s^2)}{2\ell^2}} , \tag{A.23}$$

$$_s^{\pm 1}\!\!\downarrow\!K_\ell^m \equiv \sqrt{\frac{(\ell\pm m)(\ell\pm m-1)(\ell^2-s^2)}{2\ell^2}} , \tag{A.24}$$

$$^0\lambda_\ell^m \equiv -\frac{m}{\ell} , \qquad ^{\pm 1}\lambda_\ell^m \equiv \pm\frac{1}{\ell}\sqrt{\frac{(\ell+m\mp 1+1)(\ell-m\pm 1)}{2}} .\tag{A.25}$$

We report first the link between the moments of radiation and the fluid description involving the energy density and the velocity of radiation. The link is similar for neutrinos. More details can be found in Refs. [53, 67]. Note that we define the

multipoles $\mathcal{I}_\ell^m$ from $\mathcal{I}/\bar{\mathcal{I}}$ so that it is dimensionless, and we do the same for the polarization and neutrinos multipoles. At first order we have

$$\mathcal{I}_0^{0(1)}(k) = \frac{\rho_r^{(1)}(k)}{\bar{\rho}_r}, \quad \mathcal{I}_1^{m(1)}(k) = 4v_{r,m}^{(1)}(k), \tag{A.26}$$

and at second order we obtain

$$\mathcal{I}_0^{0(2)}(\mathbf{k}) = \frac{\rho_r^{(2)}(\mathbf{k})}{\bar{\rho}_r} - 2\mathcal{K}\left\{\frac{4}{3}\sum_{n=-1}^1 (-1)^n v_{r,n}^{(1)}(\mathbf{k}_1)v_{r,-n}^{(1)}(\mathbf{k}_2)\right\}, \tag{A.27}$$

$$\mathcal{I}_1^{m(2)}(\mathbf{k}) = v_{r,m}^{(2)}(\mathbf{k}) + 2\mathcal{K}\left\{\frac{4}{3}\frac{\rho_r^{(1)}(\mathbf{k}_1)}{\bar{\rho}_r}v_{r,m}^{(1)}(\mathbf{k}_2)\right\}. \tag{A.28}$$

Note also that since $v^{i(2)} = V^{I(2)} - 2\Psi^{(1)}V^{I(1)}$ for all species [53], then

$$v_0^{(1)}(k) = V_0^{(1)}(k) = k^{(0)}V^{(1)}(k) = -kV^{(1)}(k), \tag{A.29}$$

$$v_\pm^{(1)}(k) = V_\pm^{(1)}(k) = 0, \tag{A.30}$$

$$v_0^{(2)}(k) = -kV^{(2)}(k) - 2\mathcal{K}\left\{\Psi^{(1)}(k_1)k_2^{(0)}V^{(1)}(k_2)\right\}, \tag{A.31}$$

$$v_\pm^{(2)}(k) = V_\pm^{(2)}(k) - 2\mathcal{K}\left\{\Psi^{(1)}(k_1)k_2^{(\pm)}V^{(1)}(k_2)\right\}. \tag{A.32}$$

Appendix A.2.2. First order At first order we choose to align the Fourier mode considered $\mathbf{k}$ with the direction with respect to which the moments are taken, and the dependence in $\mathbf{k}$ becomes only a dependence in its magnitude k. The set of equations obtained at first order is (dropping the obvious dependence of all quantities in η)

$$\mathcal{L}^{(1)}[\mathcal{I}]_\ell^0(k) = \mathcal{I}_\ell'^0(k) + k\left[\frac{_0^0\!\uparrow\!K_{\ell+1}^0}{2\ell+3}\mathcal{I}_{\ell+1}^0(k) - \frac{_0^0\!\downarrow\!K_\ell^0}{2\ell-1}\mathcal{I}_{\ell-1}^0(k)\right]$$
$$- \delta_\ell^0 4\Psi'(k) - \delta_\ell^1 4k\Phi(k), \tag{A.33}$$

$$\mathcal{L}^{(1)}[\mathcal{E}]_\ell^0(k) = \mathcal{E}_\ell'^0(k) + k\left[\frac{_2^0\!\uparrow\!K_{\ell+1}^0}{2\ell+3}\mathcal{E}_{\ell+1}^0(k) - \frac{_2^0\!\downarrow\!K_\ell^0}{2\ell-1}\mathcal{E}_{\ell-1}^0(k)\right], \tag{A.34}$$

$$\mathcal{C}^{(1)}[\mathcal{I}]_\ell^0(k) = \bar{\tau}'\left\{-\mathcal{I}_\ell^0(k) + \delta_\ell^0\mathcal{I}_0^0(k) + 4\delta_\ell^1 v_0(k) + \delta_\ell^2\frac{1}{10}\left[\mathcal{I}_2^0(k) - \sqrt{6}\mathcal{E}_2^0(k)\right]\right\}, \tag{A.35}$$

$$\mathcal{C}^{(1)}[\mathcal{E}]_\ell^m(k) = \bar{\tau}'\left\{-\mathcal{E}_\ell^m(k) - \delta_\ell^2\frac{\sqrt{6}}{10}\left[\mathcal{I}_2^0(k) - \sqrt{6}\mathcal{E}_2^0(k)\right]\right\}. \tag{A.36}$$

The first order magnetic modes are not excited since the first order vector and tensor modes are negligible, so we did not report them in the above equations. Additionally, the intensity and electric multipoles are only excited for $m = 0$, that is the reason why we also only reported this case.

Appendix A.2.3. Second order At second order we can only align $\mathbf{k}$ with the azimuthal direction of the moments, but not $\mathbf{k}_1$ or $\mathbf{k}_2$ at the same time. However for a first order quantity the components X_ℓ^m for a mode in a given direction $\mathbf{k}_1$ can be obtained by rotating the components X_ℓ^0 obtained when we had decided to align this direction with $\bar{\mathbf{e}}_3$. Namely this rotation leads for a mode $\mathbf{k}$ to

$$X_\ell^m(\mathbf{k}) = \sqrt{\frac{4\pi}{2\ell+1}}Y^{\star\ell m}(\mathbf{k})X_\ell^0(k), \tag{A.37}$$

and in particular for the first order velocity

$$v_n(\mathbf{k}) = -\hat{k}^{(n)} v_0(k) \, . \tag{A.38}$$

We finally obtain for the linear terms in the second order Liouville operator

$$\mathcal{L}^{(2)}[\mathcal{I}^{(2)}]_\ell^m(k) = \mathcal{I}_\ell^{'m(2)}(k) + k \left[\frac{{}_0^0{\uparrow}K_{\ell+1}^m}{2\ell+3} \mathcal{I}_{\ell+1}^{m(2)}(k) - \frac{{}_0^0{\downarrow}K_\ell^m}{2\ell-1} \mathcal{I}_{\ell-1}^{m(2)}(k) \right]$$
$$- \delta_\ell^0 \delta_m^0 4\Psi'^{(2)}(k) - \delta_\ell^1 \delta_m^0 4k\Phi^{(2)}(k)$$
$$+ \delta_\ell^2 \delta_m^1 \frac{4k}{\sqrt{3}} \Phi_1^{(2)}(k) + \delta_\ell^2 \delta_m^{-1} \frac{4k}{\sqrt{3}} \Phi_{-1}^{(2)}(k)$$
$$+ \delta_\ell^2 \delta_m^2 4H_1^{'(2)} + \delta_\ell^2 \delta_m^{-2} 4H_{-1}^{'(2)} \, , \tag{A.39}$$

$$\mathcal{L}^{(2)}[\mathcal{E}^{(2)}]_\ell^m(k) = \mathcal{E}_\ell^{'m(2)}(k) \tag{A.40}$$
$$+ k \left[\frac{{}_2^0{\uparrow}K_{\ell+1}^m}{2\ell+3} \mathcal{E}_{\ell+1}^{m(2)}(k) + \frac{2m}{\ell(\ell+1)} \mathcal{B}_\ell^{m(2)}(k) - \frac{{}_2^0{\downarrow}K_\ell^m}{2\ell-1} \mathcal{E}_{\ell-1}^{m(2)}(k) \right] \, ,$$

$$\mathcal{L}^{(2)}[\mathcal{B}^{(2)}]_\ell^m(k) = \mathcal{B}_\ell^{'m(2)}(k) \tag{A.41}$$
$$+ k \left[\frac{{}_2^0{\uparrow}K_{\ell+1}^m}{2\ell+3} \mathcal{B}_{\ell+1}^{m(2)}(k) - \frac{2m}{\ell(\ell+1)} \mathcal{E}_\ell^{m(2)}(k) - \frac{{}_2^0{\downarrow}K_\ell^m}{2\ell-1} \mathcal{B}_{\ell-1}^{m(2)}(k) \right] \, .$$

As for the quadratic terms, we obtain

$$\mathcal{L}^{(1)(1)}[\mathcal{I}]_\ell^m(k) = \mathcal{L}_{\text{time-delay}}^{(1)(1)}[\mathcal{I}]_\ell^m(k) + \mathcal{L}_{\text{lensing}}^{(1)(1)}[\mathcal{I}]_\ell^m(k)$$
$$+ 2\mathcal{K} \left\{ - \sum_{n=-1}^1 \frac{{}_0^n{\uparrow}K_{\ell+1}^m}{2\ell+3} \mathcal{I}_{\ell+1}^{m+n}(\mathbf{k}_2) 4k_1^{(-n)} \Phi(k_1) \right.$$
$$+ \sum_{n=-1}^1 \frac{{}_0^n{\downarrow}K_\ell^m}{2\ell-1} \mathcal{I}_{\ell-1}^{m-n}(\mathbf{k}_2) 4k_1^{(n)} \Phi(k_1) - 4\Psi'(k_1) \mathcal{I}_\ell^m(\mathbf{k}_2)$$
$$\left. + 4\delta_\ell^1 \left[\Psi(k_1) - \Phi(k_1) \right] \Phi(k_2) k_2^{(m)} - 8\delta_\ell^0 \Psi(k_1) \Psi'(k_2) \right\} \, , \tag{A.42}$$

with

$$\mathcal{L}_{\text{time-delay}}^{(1)(1)}[\mathcal{I}]_\ell^m(k) \equiv - 2\mathcal{K} \sum_{n=-1}^1 \frac{{}_0^n{\uparrow}K_{\ell+1}^m}{2\ell+3} \mathcal{I}_{\ell+1}^{m+n}(\mathbf{k}_2) k_2^{(-n)} \left[\Phi(k_1) + \Psi(k_1) \right]$$
$$+ 2\mathcal{K} \sum_{n=-1}^1 \frac{{}_0^n{\downarrow}K_\ell^m}{2\ell-1} \mathcal{I}_{\ell-1}^{m-n}(\mathbf{k}_2) k_2^{(n)} \left[\Phi(k_1) + \Psi(k_1) \right] \, , \tag{A.43}$$

$$\mathcal{L}_{\text{lensing}}^{(1)(1)}[\mathcal{I}]_\ell^m(k) \equiv 2\mathcal{K} \sum_{n=-1}^1 \frac{{}_0^n{\uparrow}K_{\ell+1}^m}{2\ell+3} \mathcal{I}_{\ell+1}^{m+n}(\mathbf{k}_2)(\ell+2) k_1^{(-n)} \left[\Phi(k_1) + \Psi(k_1) \right]$$
$$+ 2\mathcal{K} \sum_{n=-1}^1 \frac{{}_0^n{\downarrow}K_\ell^m}{2\ell-1} \mathcal{I}_{\ell-1}^{m-n}(\mathbf{k}_2)(\ell-1) k_1^{(n)} \left[\Phi(k_1) + \Psi(k_1) \right] \, . \tag{A.44}$$

For the electric-type polarization, we can also separate explicitely the lensing and time-delay contributions

$$
\begin{aligned}
\mathcal{L}^{(1)(1)}[\mathcal{E}]_\ell^m(k) = \mathcal{L}^{(1)(1)}_{\text{time}-\text{delay}}[\mathcal{E}]_\ell^m(k) + \mathcal{L}^{(1)(1)}_{\text{lensing}}[\mathcal{E}]_\ell^m(k) \\
+ 2\mathcal{K}\Bigg\{ - \sum_{n=-1}^{1} \frac{\frac{n}{2}{\uparrow}K_{\ell+1}^m}{2\ell+3}\mathcal{E}_{\ell+1}^{m+n}(\mathbf{k}_2)4k_1^{(-n)}\Phi(k_1) \\
+ \sum_{n=-1}^{1} \frac{\frac{n}{2}{\downarrow}K_\ell^m}{2\ell-1}\mathcal{E}_{\ell-1}^{m-n}(\mathbf{k}_2)4k_1^{(n)}\Phi(k_1) - 4\Psi'(k_1)\mathcal{E}_\ell^m(\mathbf{k}_2) \Bigg\} ,
\end{aligned} \tag{A.45}
$$

with

$$
\begin{aligned}
\mathcal{L}^{(1)(1)}_{\text{time}-\text{delay}}[\mathcal{E}]_\ell^m(k) \equiv - 2\mathcal{K} \sum_{n=-1}^{1} \frac{\frac{n}{2}{\uparrow}K_{\ell+1}^m}{2\ell+3}\mathcal{E}_{\ell+1}^{m+n}(\mathbf{k}_2)k_2^{(-n)}\left[\Phi(k_1) + \Psi(k_1)\right] \\
+ 2\mathcal{K} \sum_{n=-1}^{1} \frac{\frac{n}{2}{\downarrow}K_\ell^m}{2\ell-1}\mathcal{E}_{\ell-1}^{m-n}(\mathbf{k}_2)k_2^{(n)}\left[\Phi(k_1) + \Psi(k_1)\right] ,
\end{aligned} \tag{A.46}
$$

$$
\begin{aligned}
\mathcal{L}^{(1)(1)}_{\text{lensing}}[\mathcal{E}]_\ell^m(k) \equiv 2\mathcal{K} \sum_{n=-1}^{1} \frac{\frac{n}{2}{\uparrow}K_{\ell+1}^m}{2\ell+3}\mathcal{E}_{\ell+1}^{m+n}(\mathbf{k}_2)(\ell+2)k_1^{(-n)}\left[\Phi(k_1) + \Psi(k_1)\right] \\
+ 2\mathcal{K} \sum_{n=-1}^{1} \frac{\frac{n}{2}{\downarrow}K_\ell^m}{2\ell-1}\mathcal{E}_{\ell-1}^{m-n}(\mathbf{k}_2)(\ell-1)k_1^{(n)}\left[\Phi(k_1) + \Psi(k_1)\right] .
\end{aligned} \tag{A.47}
$$

For the magnetic-type polarization, the only contribution is coming from lensing and reads

$$
\mathcal{L}^{(1)(1)}[\mathcal{B}]_\ell^m(k) = -2\mathcal{K}\frac{2}{(\ell+1)} \sum_{n=-1}^{1} {}^n\lambda_\ell^m\, \mathcal{E}_\ell^{m-n}(\mathbf{k}_2)k_1^{(n)}\left[\Phi(k_1) + \Psi(k_1)\right] . \tag{A.48}
$$

Note that the lensing term clearly differs from Eq. (44) of Ref. [38], and this affects the results presented in Eq. (52) of Ref. [38] (and subsequently this error spreads as well into Eq. (450) of Ref. [25]). Indeed the harmonic expansion of the lensing term (7.9) should be treated as in section IV.A of Ref. [82]. There, the screen projector $S_j^i = \delta_j^i - n^i n_j$ which is implied in our notation ∇^{n^i} (see Ref. [53] for details) is not split into δ_j^i and $n^i n_j$ before performing the harmonic decomposition as done in Ref. [38], but is instead used to ensure that the object manipulated in the lensing term remains tangent to a two-dimensional sphere whose radius is parameterized by n^i. This enables to work with spinned spherical harmonics as in Ref. [82] and to derive the result almost immediately. Additionally, the multipoles of the radiation brightness ($\Delta_\ell(\mathbf{k})$ in the notation of Ref. [38]) are not rotated correctly when the azimuthal direction, with respect to which the spherical harmonics are defined, is shifted from the axis $\mathbf{k}_1$ or $\mathbf{k}_2$ of the first order calculation to the axis $\mathbf{k}$ of the second order calculation. Indeed, this change of reference axis leads to a transformation given by Eq. (A.37). Though this is taken into account correctly for the baryons velocity (for instance in the eleventh line of Eq. (44) of Ref. [38]), it is clearly forgotten for the brightness moments in the last term of the fourth line or in the last line. These two reasons explain why our treatment of quadratic terms is substantially different from Ref. [38].

Using a similar method applied to the collision term leads to

$$
\mathcal{C}^{(2)}[\mathcal{I}]_\ell^m(k) = \bar{\tau}'\left[-\mathcal{I}_\ell^{m(2)}(k) + \delta_\ell^0\delta_m^0\mathcal{I}_0^{0(2)}(k) + 4\delta_\ell^1 v_m^{(2)}(k) + \delta_\ell^2 P^{m(2)}(k)\right] , \tag{A.49}
$$

where $P^{m(2)}(k)$ is non-vanishing only if $-2 \leq m \leq 2$ and is defined in that case by

$$P^{m(2)}(k) = \frac{1}{10} \left[\mathcal{I}_2^{m(2)}(k) - \sqrt{6} \mathcal{E}_2^{m(2)}(k) \right] . \tag{A.50}$$

For the electric and magnetic type collision terms, their second order linear components read

$$\mathcal{C}^{(2)}[\mathcal{E}]_\ell^m(k) = \bar{\tau}' \left[-\mathcal{E}_\ell^{m(2)}(k) - \delta_\ell^2 \sqrt{6} P^{m(2)}(k) \right] , \tag{A.51}$$

$$\mathcal{C}^{(2)}[\mathcal{B}]_\ell^m(k) = -\bar{\tau}' \mathcal{B}_\ell^{m(2)}(k) . \tag{A.52}$$

The quadratic terms are then given by

$$\mathcal{C}^{(1)(1)}[\mathcal{I}^{(1)}]_\ell^m(k) = \tag{A.53}$$

$$2\bar{\tau}'\mathcal{K} \left\{ - \sum_{n=-1}^1 \frac{{}_0^n{\uparrow}K_{\ell+1}^m}{2\ell+3} \mathcal{I}_{\ell+1}^{m+n}(\mathbf{k}_2)v_{-n}(\mathbf{k}_1) + \sum_{n=-1}^1 \frac{{}_0^n{\downarrow}K_\ell^m}{2\ell-1} \mathcal{I}_{\ell-1}^{m-n}(\mathbf{k}_2)v_n(\mathbf{k}_1) \right.$$

$$+ \delta_\ell^0 \left[-\frac{4}{3} \sum_{n=-1}^1 (-1)^n v_n(\mathbf{k}_1)v_{-n}(\mathbf{k}_2) + \sum_{n=-1}^1 2\frac{{}_0^n{\uparrow}K_1^0}{3} \mathcal{I}_1^n(\mathbf{k}_2)v_{-n}(\mathbf{k}_1) \right]$$

$$+ \delta_\ell^1 3 \sum_{n=-1}^1 {}_0^n{\downarrow}K_1^m \mathcal{I}_0^{m-n}(\mathbf{k}_2)v_n(\mathbf{k}_1)$$

$$+ \delta_\ell^2 \sum_{n=-1}^1 \frac{{}_0^n{\downarrow}K_2^m}{3} \left[-\frac{1}{2}\mathcal{I}_1^{m-n}(\mathbf{k}_2) + 7v_{m-n}(\mathbf{k}_2) \right] v_n(\mathbf{k}_1)$$

$$\left. + \delta_\ell^3 \frac{1}{2} \sum_{n=-1}^1 \frac{{}_0^n{\downarrow}K_3^m}{5} \left[\mathcal{I}_2^{m-n}(\mathbf{k}_2) - \sqrt{6}\mathcal{E}_2^{m-n}(\mathbf{k}_2) \right] v_n(\mathbf{k}_1) \right\}$$

$$+ 2\mathcal{K} \left\{ \left[\tau'^{(1)}(\mathbf{k}_1) + \Phi^{(1)}(\mathbf{k}_1) \right] \mathcal{C}^{(1)}[\mathcal{I}^{(1)}]_\ell^m(\mathbf{k}_2) \right\} ,$$

$$\mathcal{C}^{(1)(1)}[\mathcal{E}^{(1)}]_\ell^m(k) = \tag{A.54}$$

$$2\bar{\tau}'\mathcal{K} \left\{ - \sum_{n=-1}^1 \frac{{}_2^n{\uparrow}K_{\ell+1}^m}{2\ell+3} \mathcal{E}_{\ell+1}^{m+n}(\mathbf{k}_2)v_{-n}(\mathbf{k}_1) + \sum_{n=-1}^1 \frac{{}_2^n{\downarrow}K_\ell^m}{2\ell-1} \mathcal{E}_{\ell-1}^{m-n}(\mathbf{k}_2)v_n(\mathbf{k}_1) \right.$$

$$+ \delta_\ell^2 \sum_{n=-1}^1 \frac{{}_0^n{\downarrow}K_2^m}{3} \left[\frac{\sqrt{6}}{2}\mathcal{I}_1^{m-n}(\mathbf{k}_2) - \sqrt{6}v_{m-n}(\mathbf{k}_2) \right] v_n(\mathbf{k}_1)$$

$$\left. + \delta_\ell^3 \frac{1}{2} \sum_{n=-1}^1 \frac{{}_2^n{\downarrow}K_3^m}{5} \left[-\sqrt{6}\mathcal{I}_2^{m-n}(\mathbf{k}_2) + 6\mathcal{E}_2^{m-n}(\mathbf{k}_2) \right] v_n(\mathbf{k}_1) \right\}$$

$$+ 2\mathcal{K} \left\{ \left[\tau'^{(1)}(\mathbf{k}_1) + \Phi^{(1)}(\mathbf{k}_1) \right] \mathcal{C}^{(1)}[\mathcal{E}^{(1)}]_\ell^m(\mathbf{k}_2) \right\} ,$$

$$\mathcal{C}^{(1)(1)}[\mathcal{B}^{(1)}]_\ell^m(k) = 2\bar{\tau}'\mathcal{K} \left\{ \frac{-2}{(\ell+1)} \sum_{n=-1}^1 {}^n\lambda_\ell^m v_n(\mathbf{k}_1)\mathcal{E}_\ell^{m-n}(\mathbf{k}_2) \right. \tag{A.55}$$

$$\left. - \delta_\ell^2 \sum_{n=-1}^1 {}^n\lambda_2^m v_n(\mathbf{k}_1) \left[\frac{4}{5}\mathcal{E}_2^{m-n}(\mathbf{k}_2) - \frac{2}{15}\sqrt{6}\mathcal{I}_2^{m-n}(\mathbf{k}_2) \right] \right\} .$$

Appendix A.3. Fluid equations

For baryons and cold dark matter we only need the two first moments, that is the continuity and Euler equations, since there is no anisotropic stress. The continuity equations are

$$\left[\frac{\rho^{(1)}(k)}{\bar{\rho}}\right]' + kv_0^{(1)}(k) - 3\Psi^{'(1)}(k) = 0\,, \tag{A.56}$$

$$\left[\frac{\rho^{(2)}(k)}{\bar{\rho}}\right]' + kv_0^{(2)}(k) - 3\Psi^{'(2)}(k)$$

$$+2\mathcal{K}\left\{-\sum_{n=-1}^{1}(-1)^n\left[\mathcal{H}v_n(\mathbf{k}_1)v_{-n}(\mathbf{k}_2) + \frac{\rho(\mathbf{k}_1)}{\bar{\rho}}k_1^{(n)}v_{-n}(\mathbf{k}_2) + 2v_n(\mathbf{k}_1)v'_{-n}(\mathbf{k}_2)\right]\right.$$

$$+\left[\frac{\rho(k_1)}{\bar{\rho}} + \Phi(k_1) + \Psi(k_1)\right]k_2v_0(k_2) - 3\Psi'(k_1)\frac{\rho(k_2)}{\bar{\rho}} - 6\Psi(k_1)\Psi'(k_2)$$

$$\left.-2\sum_{n=-1}^{1}(-1)^n\left[\Phi(k_2) - \Psi(k_2)\right]k_2^{(n)}v_{-n}(\mathbf{k}_1)\right\}$$

$$= -\frac{2\bar{\tau}'}{R}\mathcal{K}\left\{\sum_{n=-1}^{1}(-1)^n\left[\frac{1}{4}\mathcal{I}_1^n(\mathbf{k}_2)v_{-n}(\mathbf{k}_1) - v_n(\mathbf{k}_1)v_{-n}(\mathbf{k}_2)\right]\right\}\,. \tag{A.57}$$

The Euler equation reads

$$v_m^{'(1)}(k) + \mathcal{H}v_m^{(1)}(k) - \delta_m^0 k\Phi^{(1)}(k) = -\frac{\bar{\tau}'}{3R}\left[-\mathcal{I}_1^{m(1)}(k) + 4v_m^{(1)}(k)\right]\,, \tag{A.58}$$

$$v_m^{'(2)}(k) + \mathcal{H}v_m^{(2)}(k) - \delta_m^0 k\Phi^{(2)}(k) \tag{A.59}$$

$$+2\mathcal{K}\left\{\left[\frac{\rho(k_1)}{\bar{\rho}} - \Phi(k_1)\right][v'_m(\mathbf{k}_2) + \mathcal{H}v_m(\mathbf{k}_2)] + \left[\frac{\rho(k_1)}{\bar{\rho}} + \Psi(k_1)\right]k_2^{(m)}\Phi(k_2)\right.$$

$$+v_m(\mathbf{k}_2)\left[\left(\frac{\rho(k_1)}{\bar{\rho}}\right)' - 4\Psi'(k_1)\right] + \delta_m^0 k\Phi(k_1)\Phi(k_2) + kv_m(\mathbf{k}_2)v_0(\mathbf{k}_1)\right\}$$

$$= -\frac{\bar{\tau}'}{4R}\left[-\mathcal{I}_1^{m(2)}(k) + 4v_m^{(2)}(k)\right] - \frac{1}{2R}\mathcal{K}\left\{\tau^{'(1)}(\mathbf{k}_1)\left[-\mathcal{I}_1^{m(1)}(\mathbf{k_2}) + 4v_m^{(1)}(\mathbf{k_2})\right]\right\}$$

$$-\frac{1}{2R}\bar{\tau}'\mathcal{K}\left\{4\mathcal{I}_0^0(\mathbf{k}_2)v_m(\mathbf{k}_1) - \sum_{n=-1}^{1}\frac{{}_0^n\!\uparrow\!K_2^m}{5}\mathcal{I}_2^{m+n}(\mathbf{k}_2)v_{-n}(\mathbf{k}_1)\right\}\,.$$

In the case of cold dark matter, the right hand side of all these equations vanishes since it is collisionless.

Appendix A.4. Perturbed recombination

The fraction of free electron at the background level is obtained from a Boltzmann equation where the collision term encodes all the relevant processes in the recombination. We shall not detail any of it here and it can be found in Refs. [50, 70, 91, 92] (see also the different method of Ref. [93]). Since the interaction rate is given by $\tau' \equiv ax_e n_e \sigma_T$, where n_e is the number density of electrons (free and

non-free), σ_{T} the Thomson cross-section, and x_{e} the fraction of free electrons, its perturbation is given by

$$\tau'^{(1)} = \bar{\tau}' \left(\frac{n_{\mathrm{e}}^{(1)}}{\bar{n}_{\mathrm{e}}} + \frac{x_{\mathrm{e}}^{(1)}}{\bar{x}_{\mathrm{e}}} \right) . \tag{A.60}$$

Since electrons and baryons are tightly coupled through Compton interactions and collisions [50],

$$\frac{n_{\mathrm{e}}^{(1)}}{\bar{n}_{\mathrm{e}}} = \frac{n_{\mathrm{b}}^{(1)}}{\bar{n}_{\mathrm{b}}} . \tag{A.61}$$

As for the fraction of free electrons, at the background level it obeys

$$\bar{x}_{\mathrm{e}}' + 3H\bar{x}_{\mathrm{e}} = \bar{Q} , \tag{A.62}$$

where the expression of Q can be found in Ref. [50] (more precisely what is called Q in this reference is equivalent to $n_{\mathrm{e}}Q$ in here). It is in general a function of $(x_{\mathrm{e}}, n_{\mathrm{e}}, T, H)$. T is the temperature of baryons and photons since it is approximately the same around recombination [50]. H is the local divergence of baryons ($H \equiv \nabla_\mu u_{\mathrm{b}}^\mu/3$) which at the background is the Hubble factor (in cosmic time). $\bar{Q}$ is obtained by taking the background value of all its arguments, that is

$$\bar{Q} = Q(\bar{x}_{\mathrm{e}}, \bar{n}_{\mathrm{e}}, \bar{T}, \bar{H}) . \tag{A.63}$$

We report on Fig. A1 the numerical results obtained for the background fraction of free electrons. This has to be compared to the results obtained with RECFAST [94, 95] since we have implemented the correction to the three-level atom approximation implemented in this code, that is using its fudge factor of 1.14 for the last stages of the Hydrogen recombination and the fudge factor 0.86 for the HeI recombination.
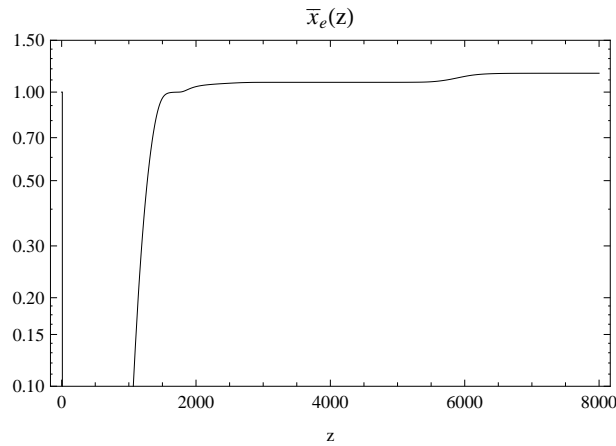
Figure A1. Evolution of the free electrons fraction as a function of the redshift. We can see the transition of HeII and HeI at approximately z=6000 and z=2500 respectively, and then the recombination of Hydrogen around z=1000.

At first order, the evolution of the fraction of free electrons reads [50] simply

$$\left(\frac{x_{\mathrm{e}}^{(1)}}{\bar{x}_{\mathrm{e}}} \right)' = \Phi^{(1)}\bar{Q} + Q^{(1)} . \tag{A.64}$$

The perturbation $Q^{(1)}$ is obained by taking the first order of $Q(x_e, n_e, T, H)$ which is obtained by partial differentiation with respect to all the arguments of Q. The quantity $H^{(1)}$ is given by

$$aH^{(1)} = -\mathcal{H}\Phi^{(1)} - \frac{1}{3}\left(\frac{n_b^{(1)}}{\bar{n}_b}\right)' . \tag{A.65}$$

The enhancement due to the perturbations in the fraction of free electrons is plotted in Fig. A2.
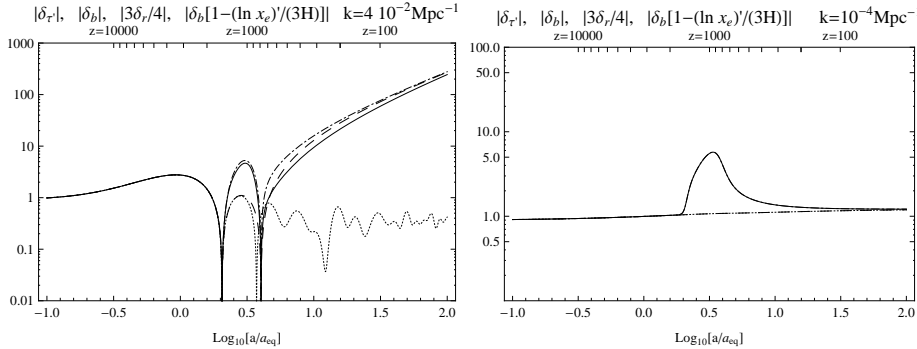
Figure A2. Enhancement of the interaction rate due to the perturbations in the fraction of free electrons. $\delta_{\tau'}$, δ_b and δ_r are respectively the relative perturbation of τ', n_e and ρ_r. We plot $\delta_{\tau'}$ in continuous line, and δ_b in dashed line. According to Eq. (A.60), the difference between the two is the enhancement due to perturbed recombination. This has to be compared to the large scale limit of the delayed recombination $\delta_b[1 - 1/3(\ln x_e)'/\mathcal{H}]$, which is plotted in dashed-dotted line. We also plot in dotted line $3\delta_r/4$ to show the departure from tight coupling around recombination. We have considered the two cases $k = 10^{-4}\,\mathrm{Mpc}^{-1}$ (right) and $k = 0.04\,\mathrm{Mpc}^{-1}$ (left).

Appendix B. Emitting sources

In the line of sight approach, we need to define the emitting sources. Instead of working with the brightness $\mathcal{I}$ and its corresponding electric and magnetic type polarizations $\mathcal{E}$ and $\mathcal{B}$, we work with Θ (defined in Eq. (4.1)), $\tilde{\mathcal{E}} \equiv \mathcal{E}/(4\bar{\mathcal{I}})$ and $\tilde{\mathcal{B}} \equiv \mathcal{B}/(4\bar{\mathcal{I}})$. They are expanded similarly to Eq. (A.21). We obtain at first order

$$S_{\Theta,\ell}^{0(1)}(k) \equiv \delta_\ell^0 \Psi'(k) + \delta_\ell^1 k\Phi(k) + \frac{1}{4}\left[\mathcal{C}^{(1)}[\mathcal{I}]_\ell^0(k) + \bar{\tau}'\mathcal{I}_\ell^{0(1)}(k)\right] , \tag{B.1}$$

$$S_{\tilde{\mathcal{E}},\ell}^{0(1)}(k) \equiv \frac{1}{4}\mathcal{C}^{(1)}[\mathcal{E}]_\ell^0(k) . \tag{B.2}$$

However, if we want to have all effects but the late ISW localized on the last scattering surface, we need to integrate by parts in the line of sight integral solution. This boils down to using instead

$$S_{\Theta,\ell}^{0(1)}(k) \equiv \delta_\ell^0 \left[\Psi'(k) + \Phi'(k)\right] + \delta_\ell^0 \bar{\tau}'\Phi(k)\left[\mathcal{C}^{(1)}[\mathcal{I}]_\ell^0(k) + \bar{\tau}'\mathcal{I}_\ell^{0(1)}(k)\right] . \tag{B.3}$$

At second order the sources are

$$S_{\Theta,\ell}^{m(2)}(k) \equiv \delta_\ell^0 \delta_m^0 \left[\Phi'^{(2)} + \Psi'^{(2)}(k)\right] + \delta_\ell^0 \delta_m^0 \bar\tau' \Phi^{(2)}(k) \tag{B.4}$$

$$- \delta_\ell^2 \delta_m^1 \frac{k}{\sqrt{3}} \Phi_1^{(2)}(k) - \delta_\ell^2 \delta_m^{-1} \frac{k}{\sqrt{3}} \Phi_{-1}^{(2)}(k) - \delta_\ell^2 \delta_m^2 H_1^{'(2)}$$

$$- \delta_\ell^2 \delta_m^{-2} H_{-1}^{'(2)} + \frac{1}{4}\left[\mathcal{C}^{(2)}[\mathcal{I}]_\ell^m(k) + \bar\tau' \mathcal{I}_\ell^{m(2)}(k)\right],$$

$$S_{\tilde{\mathcal{E}},\ell}^{m(2)}(k) \equiv \frac{1}{4}\left[\mathcal{C}^{(2)}[\mathcal{E}]_\ell^m(k) + \bar\tau' \mathcal{E}_\ell^{m(2)}(k)\right] \tag{B.5}$$

$$S_{\tilde{\mathcal{B}},\ell}^{m(2)}(k) \equiv \frac{1}{4}\left[\mathcal{C}^{(2)}[\mathcal{B}]_\ell^m(k) + \bar\tau' \mathcal{B}_\ell^{m(2)}(k)\right], \tag{B.6}$$

$$S_{\Theta,\ell}^{m(1)(1)}(k) \equiv \frac{1}{4}\mathcal{C}^{(1)(1)}[\mathcal{I}]_\ell^m(k) - \frac{1}{4}\mathcal{L}^{(1)(1)}[\mathcal{I}]_\ell^m(k), \tag{B.7}$$

$$S_{\tilde{\mathcal{E}},\ell}^{m(1)(1)}(k) \equiv \frac{1}{4}\mathcal{C}^{(1)(1)}[\mathcal{E}]_\ell^m(k) - \frac{1}{4}\mathcal{L}^{(1)(1)}[\mathcal{E}]_\ell^m(k), \tag{B.8}$$

$$S_{\tilde{\mathcal{B}},\ell}^{m(1)(1)}(k) \equiv \frac{1}{4}\mathcal{C}^{(1)(1)}[\mathcal{B}]_\ell^m(k) - \frac{1}{4}\mathcal{L}^{(1)(1)}[\mathcal{B}]_\ell^m(k). \tag{B.9}$$

Appendix C. Quadrupole initial conditions

Since $\mathcal{H} \sim 1/\eta$ in the radiation era, we need to determine the initial conditions for $\mathcal{N}_2^0$ up to terms in $(k\eta_{\text{init}})^2$, and thus to know the initial conditions for $\mathcal{N}_1^m$ up to terms of order $k\eta_{\text{init}}$. In fact, deep in the radiation dominated era, $\mathcal{N}_\ell^{0(1)} \sim (k\eta)^\ell$.

$$\mathcal{I}_1^{0(1)}(k) = \mathcal{N}_1^{0(1)}(k) = \frac{2k}{\mathcal{H}}\Phi^{(1)}(k), \tag{C.1}$$

$$\mathcal{I}_1^{0(2)}(k) = \mathcal{N}_1^{0(2)}(k) = \frac{2k}{\mathcal{H}}\Phi^{(2)}(k) - \mathcal{K}\left\{\frac{8k}{\mathcal{H}}\Phi^{(1)}(\mathbf{k}_1)\Phi^{(1)}(\mathbf{k}_2)\right\}. \tag{C.2}$$

Using this, we deduce from the Boltzmann equation that at first order [70]

$$\mathcal{N}_2^{0(1)}(k) = \frac{2k^2}{3\mathcal{H}^2}\Phi^{(1)}. \tag{C.3}$$

At second order we obtain the following initial condition

$$\mathcal{N}_2^{0(2)}(k) = \frac{2k^2}{3\mathcal{H}^2}\Phi^{(2)}(k) + S_5 \tag{C.4}$$

with

$$S_5 = -\mathcal{K}\left\{\frac{8k^2}{3\mathcal{H}^2}\Phi^{(1)}(\mathbf{k}_1)\Phi^{(1)}(\mathbf{k}_2)\right\} - \frac{1}{2\mathcal{H}}\mathcal{L}^{\#(1)(1)}[\mathcal{N}]_2^0(k) \tag{C.5}$$

$$= -\mathcal{K}\left\{\frac{8k^2}{3\mathcal{H}^2}\Phi^{(1)}(\mathbf{k}_1)\Phi^{(1)}(\mathbf{k}_2) + \frac{2k_1^2}{3\mathcal{H}^2}\Phi^{(1)}(\mathbf{k}_1)\Phi^{(1)}(\mathbf{k}_2)\right.$$

$$\left. - \sum_{n=-1}^{1}\frac{\,_0^n\rfloor K_2^0}{6\mathcal{H}}\mathcal{N}_1^{-n(1)}(\mathbf{k}_2)\left[5k_1^{(n)}\Phi^{(1)}(\mathbf{k}_1) + (k_2^{(n)} + k_1^{(n)})\Psi^{(1)}(\mathbf{k}_1)\right]\right\}.$$

As for radiation, though the anisotropic stress is vanishing at initial time due to the high collision rate, the moment for $\ell = 2$ is not vanishing since the bulk motion of radiation has a quadrupole [53, 67, 90]. We deduce that at initial time

$$
\mathcal{I}_2^{0(2)}(k) = \mathcal{K} \left\{ \frac{20}{3} \sum_{n=-1}^{1} {}_0^n \lfloor K_2^0 \frac{\mathcal{I}_1^{n(1)}(\mathbf{k}_1)}{4} \frac{\mathcal{I}_1^{-n(1)}(\mathbf{k}_2)}{4} \right\}
$$

$$
= \mathcal{K} \left\{ \frac{5}{3\mathcal{H}^2} \sum_{n=-1}^{1} {}_0^n \lfloor K_2^0 \, k_1^n k_2^{-n} \Phi^{(1)}(k_1) \Phi^{(1)}(k_2) \right\} . \tag{C.6}
$$

Appendix D. Closure relations for vector and tensor modes

We reproduce here the closure relations needed to integrate the Boltzmann equation for the vector and tensor modes. They are derived in Eqs. (5.4.48) and (5.4.49) of Ref. [79] which is not easily available. They correspond to the equations satisfied by the last multipoles in brightness and polarization kept in the truncated Boltzmann hierarchy. At first order we need only to retain the scalar closure relation ($m = 0$). However at second order we have to consider also the vector and tensor parts ($m = 1, 2$). Note that the presence of quadratic terms at second order implies that these closure relations are not necessarily accurate as they were derived for the linear Boltzmann equation. For the brightness part, the closure relation reads

$$
\mathcal{I}_\ell^{m\prime} = k \left[\sqrt{\frac{l + |m|}{\ell - |m|}} \frac{(2\ell + 1)}{(2\ell - 1)} \mathcal{I}_{\ell-1}^m - \frac{\ell + 1 + |m|}{k\eta} \mathcal{I}_\ell^m \right] . \tag{D.1}
$$

For the polarization part, the closure relation for $\mathcal{E}_\ell^m$ and $\mathcal{B}_\ell^m$ is deduced by taking the real and imaginary part of

$$
(\mathcal{E}_\ell^m + \mathrm{i}\mathcal{B}_\ell^m)' = k \left[\sqrt{1 - \frac{m^2}{\ell^2}} \sqrt{\frac{l + 2}{\ell - 2}} \frac{(2\ell + 1)}{(2\ell - 1)} \left(\mathcal{E}_{\ell-1}^m + \mathrm{i}\mathcal{B}_{\ell-1}^m \right) - \frac{\ell + 3}{k\eta} \left(\mathcal{E}_\ell^m + \mathrm{i}\mathcal{B}_\ell^m \right) \right.
$$

$$
\left. + \mathrm{i}\frac{m}{\ell} \left(\mathcal{E}_\ell^m + \mathrm{i}\mathcal{B}_\ell^m \right) \right] . \tag{D.2}
$$

References

[1] E. Komatsu *et al.*, (2010), [arXiv:1001.4538].
[2] Planck, http://www.rssd.esa.int/.
[3] W. Hu and N. Sugiyama, Astrophys. J. **444**, 489 (1995), [arXiv:astro-ph/9407093].
[4] W. Hu and N. Sugiyama, Phys. Rev. D **51**, 2599 (1995), [arXiv:astro-ph/9411008].
[5] V. Mukhanov, H. Feldman, and R. Brandenberger, Phys. Rep. **215**, 203 (1992).
[6] A. Linde, Lect. Notes Phys. **738**, 1 (2008), [arXiv:0705.0164].
[7] S. Dodelson, *Modern cosmology* (2003).
[8] V. Mukhanov, *Physical Foundations of Cosmology* (2005).
[9] F. Bernardeau, *Cosmologie* (EDP Science, Paris, France, 2008).
[10] P. Peter and J.-P. Uzan, *Primordial Cosmology* (Oxford University Press, Oxford, UK, 2009).
[11] R. Durrer, *The Cosmic Microwave Background* (Cambridge University Press, 2008).
[12] S. Weinberg, *Cosmology* (Oxford University Press, 2008).
[13] J. Maldacena, JHEP **0305**, 013 (2003), [arXiv:astro-ph/0210603].
[14] M. Alishahiha, E. Silverstein, and D. Tong, Phys. Rev. D **70**, 123505 (2004), [arXiv:hep-th/0404084].
[15] F. Bernardeau and J.-P. Uzan, Phys. Rev. D **66**, 103506 (2002), [arXiv:hep-ph/0207295].
[16] E. Komatsu, *The Pursuit of Non-Gaussian Fluctuations in the Cosmic Microwave Background*, PhD thesis, Tohoku University, 2002, [arXiv:astro-ph/0206039].

[17] N. Bartolo, S. Matarrese, and A. Riotto, Phys. Rev. D **65**, 103505 (2002), [`arXiv:hep-ph/0112261`].
[18] F. Bernardeau and J.-P. Uzan, Phys. Rev. D **67**, 121301 (2003), [`arXiv:astro-ph/0209330`].
[19] F. Bernardeau, T. Brunier, and J.-P. Uzan, (2006), [`arXiv:astro-ph/0604200`].
[20] G. I. Rigopoulos, E. P. S. Shellard, and B. J. W. van Tent, Phys. Rev. D **73**, 083522 (2006), [`arXiv:astro-ph/0506704`].
[21] M. Sasaki, Progress of Theoretical Physics **120**, 159 (2008), [`arXiv:0805.0974`].
[22] J. R. Bond, A. V. Frolov, Z. Huang, and L. Kofman, Physical Review Letters **103**, 071301 (2009), [`arXiv:0903.3407`].
[23] N. Bartolo, E. Komatsu, S. Matarrese, and A. Riotto, Phys. Rep. **402**, 103 (2004), [`arXiv:astro-ph/0406398`].
[24] E. Komatsu *et al.*, Non-Gaussianity as a Probe of the Physics of the Primordial Universe and the Astrophysics of the Low Redshift Universe, in *The Astronomy and Astrophysics Decadal Survey*, Astronomy Vol. 2010, pp. 158–+, 2009, [`arXiv:0902.4759`].
[25] N. Bartolo, S. Matarrese, and A. Riotto, (2010), [`arXiv:1001.3957`].
[26] N. Bartolo, S. Matarrese, and A. Riotto, JHEP **0404**, 006 (2004), [`arXiv:astro-ph/0308088`].
[27] T. Pyne and S. M. Carroll, Phys. Rev. D **53**, 2920 (1996), [`arXiv:astro-ph/9510041`].
[28] S. Mollerach and S. Matarrese, Phys. Rev. D **56**, 4494 (1997), [`arXiv:astro-ph/9702234`].
[29] D. M. Goldberg and D. N. Spergel, Phys. Rev. D **59**, 103002 (1999), [`arXiv:astro-ph/9811251`].
[30] E. Komatsu and D. N. Spergel, Phys. Rev. D **63**, 063002 (2001), [`arXiv:astro-ph/0005036`].
[31] D. Babich, P. Creminelli, and M. Zaldarriaga, JCAP **0408**, 009 (2004), [`arXiv:astro-ph/0405356`].
[32] N. Bartolo, S. Matarrese, and A. Riotto, Phys. Rev. Lett. **93**, 231301 (2004), [`arXiv:astro-ph/0407505`].
[33] E. Komatsu, D. N. Spergel, and B. D. Wandelt, Astrophys. J. **634**, 14 (2005), [`arXiv:astro-ph/0305189`].
[34] M. Liguori, F. K. Hansen, E. Komatsu, S. Matarrese, and A. Riotto, Phys. Rev. D **73**, 043505 (2006), [`arXiv:astro-ph/0509098`].
[35] N. Bartolo and A. Riotto, JCAP **0903**, 017 (2009), [`arXiv:0811.4584`].
[36] R. Khatri and B. D. Wandelt, Phys. Rev. **D79**, 023501 (2009), [`arXiv:0810.4370`].
[37] L. Senatore, S. Tassev, and M. Zaldarriaga, (2008), [`arXiv:0812.3658`].
[38] D. Nitta, E. Komatsu, N. Bartolo, S. Matarrese, and A. Riotto, JCAP **0905**, 014 (2009), [`arXiv:0903.0894`].
[39] D. Hanson, K. M. Smith, A. Challinor, and M. Liguori, (2009), [`arXiv:0905.4732`].
[40] L. Boubekeur, P. Creminelli, G. D'Amico, J. Norena, and F. Vernizzi, (2009), [`arXiv:0906.0980`].
[41] A. Mangilli and L. Verde, (2009), [`arXiv:0906.2317`].
[42] M. Liguori, E. Sefusatti, J. R. Fergusson, and E. P. S. Shellard, (2010), [`arXiv:1001.4707`].
[43] T. Okamoto and W. Hu, Phys. Rev. **D66**, 063008 (2002), [`arXiv:astro-ph/0206155`].
[44] N. Kogo and E. Komatsu, Phys. Rev. **D73**, 083007 (2006), [`arXiv:astro-ph/0602099`].
[45] F. Bernardeau, T. Brunier, and J.-P. Uzan, Phys. Rev. D **69**, 063520 (2004), [`arXiv:astro-ph/0311422`].
[46] S. Weinberg, Phys. Rev. D **72**, 043514 (2005), [`arXiv:hep-th/0506236`].
[47] S. Weinberg, Phys. Rev. D **74**, 023508 (2006), [`arXiv:hep-th/0605244`].
[48] S. Weinberg, Phys. Rev. D **78**, 063534 (2008), [`arXiv:0805.3781`].
[49] C. Pitrou, J.-P. Uzan, and F. Bernardeau, Phys. Rev. D **78**, 063526 (2008), [`arXiv:0807.0341`].
[50] L. Senatore, S. Tassev, and M. Zaldarriaga, JCAP **0908**, 031 (2009), [`arXiv:0812.3652`].
[51] R. Khatri and B. D. Wandelt, Phys. Rev. **D79**, 023501 (2009), [`arXiv:0810.4370`].
[52] K. Nakamura, Prog. Theor. Phys. **117**, 17 (2007), [`arXiv:gr-qc/0605108`].
[53] C. Pitrou, Class. Quant. Grav. **26**, 065006 (2009), [`arXiv:0809.3036`].
[54] C. Pitrou, The radiative transfer for polarized radiation at second order in cosmological perturbations, 2008, [`arXiv:0809.3245`].
[55] N. Bartolo, S. Matarrese, and A. Riotto, JCAP **0508**, 010 (2005), [`arXiv:astro-ph/0506410`].
[56] N. Aghanim, S. Majumdar, and J. Silk, Reports on Progress in Physics **71**, 066902 (2008), [`arXiv:0711.0518`].
[57] C. Pitrou, F. Bernardeau, and J.-P. Uzan, (2009), [`arXiv:arXiv:0912.3655`].
[58] C. Pitrou, `http://icg.port.ac.uk/~pitrouc/cmbquick.htm`.
[59] M. Bruni, S. Matarrese, S. Mollerach, and S. Sonego, Class. Quant. Grav. **14**, 2585 (1997), [`arXiv:gr-qc/9609040`].
[60] WMAP, E. Komatsu *et al.*, Astrophys. J. Suppl. **180**, 330 (2009), [`arXiv:0803.0547`].
[61] J. Lesgourgues and S. Pastor, Phys. Rept. **429**, 307 (2006), [`arXiv:astro-ph/0603494`].

[62] I. Tereno *et al.*, Astron. Astrophys. **500**, 657 (2009), [`arXiv:0810.0555`].

[63] W. Hu and M. White, Phys. Rev. D **56**, 596 (1997), [`arXiv:astro-ph/9702170`].

[64] A. Coc, K. A. Olive, J.-P. Uzan, and E. Vangioni, Phys. Rev. **D79**, 103512 (2009), [`arXiv:0811.1845`].

[65] M. Bucher, K. Moodley, and N. Turok, (2000), [`arXiv:astro-ph/0011025`].

[66] A. Linde and V. Mukhanov, Phys. Rev. D **56**, 535 (1997), [`arXiv:astro-ph/9610219`].

[67] C. Pitrou, Class. Quant. Grav. **24**, 6127 (2007), [`arXiv:0706.4383`].

[68] K. A. Malik and D. Wands, Class. Quant. Grav. **21**, L65 (2004), [`arXiv:astro-ph/0307055`].

[69] F. Vernizzi, Phys. Rev. D **71**, 061301 (2005), [`arXiv:astro-ph/0411463`].

[70] C.-P. Ma and E. Bertschinger, Astrophys. J. **455**, 7 (1995), [`arXiv:astro-ph/9506072`].

[71] P. Creminelli, A. Nicolis, L. Senatore, M. Tegmark, and M. Zaldarriaga, JCAP **0605**, 004 (2006), [`arXiv:astro-ph/0509029`].

[72] P. Creminelli, L. Senatore, M. Zaldarriaga, and M. Tegmark, JCAP **0703**, 005 (2007), [`arXiv:astro-ph/0610600`].

[73] M. Zaldarriaga and U. Seljak, Phys. Rev. D **55**, 1830 (1997), [`arXiv:astro-ph/9609170`].

[74] W. Hu and M. White, New Astron. **2**, 323 (1997), [`arXiv:astro-ph/9706147`].

[75] W. Hu, U. Seljak, M. J. White, and M. Zaldarriaga, Phys. Rev. D **57**, 3290 (1998), [`arXiv:astro-ph/9709066`].

[76] C. Pitrou, J.-P. Uzan, and F. Bernardeau, (2010).

[77] L. R. Abramo and T. S. Pereira, (2010), [`arXiv:1002.3173`].

[78] S. Prunet, J.-P. Uzan, F. Bernardeau, and T. Brunier, Phys. Rev. **D71**, 083508 (2005), [`arXiv:astro-ph/0406364`].

[79] A. Riazuelo, *Signature de divers modèles d'univers primordial dans les anisotropies du rayonnement fossile*, PhD thesis, Université Paris Sud, 2000.

[80] E. Fenu, C. Pitrou, and R. Maartens.

[81] R. Khatri and B. D. Wandelt, (2009), [`arXiv:0903.0871`].

[82] W. Hu, Phys. Rev. D **62**, 043007 (2000), [`arXiv:astro-ph/0001303`].

[83] N. Bartolo, S. Matarrese, and A. Riotto, JCAP **0606**, 024 (2006), [`arXiv:astro-ph/0604416`].

[84] M. Zaldarriaga, Phys. Rev. **D62**, 063510 (2000), [`arXiv:astro-ph/9910498`].

[85] A. Lewis and A. Challinor, Phys. Rept. **429**, 1 (2006), [`arXiv:astro-ph/0601594`].

[86] D. N. Spergel and D. M. Goldberg, Phys. Rev. D **59**, 103001 (1999), [`arXiv:astro-ph/9811252`].

[87] L. Verde and D. N. Spergel, Phys. Rev. D **65**, 043007 (2002), [`arXiv:astro-ph/0108179`].

[88] W. Hu and A. Cooray, Phys. Rev. **D63**, 023504 (2001), [`arXiv:astro-ph/0008001`].

[89] V. Acquaviva, N. Bartolo, S. Matarrese, and A. Riotto, Nucl. Phys. B **667**, 119 (2003), [`arXiv:astro-ph/0209156`].

[90] N. Bartolo, S. Matarrese, and A. Riotto, JCAP **0701**, 019 (2007), [`arXiv:astro-ph/0610110`].

[91] P. J. E. Peebles and J. T. Yu, Astrophys. J. **162**, 815 (1970).

[92] A. Lewis and A. Challinor, Phys. Rev. **D76**, 083005 (2007), [`arXiv:astro-ph/0702600`].

[93] B. Novosyadlyj, Mon. Not. Roy. Astron. Soc. **370**, 1771 (2006), [`arXiv:astro-ph/0603674`].

[94] S. Seager, D. D. Sasselov, and D. Scott, Astrophys. J. **523**, L1 (1999), [`arXiv:astro-ph/9909275`].

[95] W. Y. Wong, A. Moss, and D. Scott, (2007), [`arXiv:0711.1357`].